Doctoral Thesis

Galactic Chemical Evolution: Estimating the Fuel Supply Rate on the Galactic Disk from High-velocity Cloud (HVC) Infall

Kwang Hyun Sung

Department of Physics

Graduate School of UNIST

2020

Galactic Chemical Evolution: Estimating the Fuel Supply Rate on the Galactic Disk from High-velocity Cloud (HVC) Infall

Kwang Hyun Sung

Department of Physics

Graduate School of UNIST

Galactic Chemical Evolution: Estimating the Fuel Supply Rate on the Galactic Disk from High-velocity Cloud (HVC) Infall

A dissertation
submitted to the Graduate School of UNIST
in partial fulfillment of the
requirements for the degree of
Doctor of Philosophy

Kwang Hyun Sung

12. 13. 2019 Month/Day/Year of submission
Approved by

Advisor
Kyujin Kwak

Galactic Chemical Evolution: Estimating the Fuel Supply Rate on the Galactic Disk from High-velocity Cloud (HVC) Infall

Kwang Hyun Sung

This certifies that the dissertation of Kwang Hyun Sung is approved.

12. 13. 2019 Month/Day/Year of submission

Advisor: Kyujin Kwak

Dongsu Ryu

Chang-Hwan Lee

Min Sup Hur

Moses Chung

Acknowledgements

First and foremost, I want to thank my advisor, Prof. Kyujin Kwak for helping me understand that my work can be meaningful in its own way. I also want to say thank you to my father who has always given me many pieces of advice as an expert in his field. Looking up to them, I was able to see what it is to be a true scholar and how much effort it takes to reach such level. My wife has quit her job knowing that she needed to stay right next to me throughout the whole process and I am hoping for a chance to return everything that she has done for me. In fact, my whole family has been supporting me all the way and I would like them to know that it was their love that kept me on my feet. At last, I truly wish everybody in academia to be successful in their research so that the world we live in would ever expand.

Abstract

Driven by the stellar nucleosynthesis over numerous generations of stars, Galactic Chemical Evolution (GCE) is the proportional buildup of helium and heavier elements within a galaxy. The most evident way to reveal the history of the galactic chemical composition and distribution is to search for the stars with a very long lifetime which would serve as fossils carrying information of the chemical abundances at the time the stars were born. However, a job of collecting a good amount of stars enough to explain the complete evolution history of the chemical abundance in a galaxy is nearly impossible to accomplish. Therefore, instead of looking for fossils, previous studies focused on developing an alternative method which is to build an analytical model from the basic knowledge of physics and our galaxy. One of the first GCE models to be developed was the Simple Model of galactic chemical evolution. The history of chemical enrichment in closed systems such as the galactic bulge was fairly well reconstructed through the model. However, when applied to the nearby solar system, the number of low-metal stars were overpredicted compared to the observed number of stars. Soon after, it was proved that allowing low-metal gas inflow could be one of the solutions to such discrepancy between the model prediction and real observation and the infall rate of ~ 0.45 $M_{\odot}yr^{-1}$ was suggested from GCE models. Later discovered through the 21 cm radio emission line, High Velocity Clouds (HVCs) with the deviation velocities over 90 km/s are considered a good supply of metal-poor gas as the estimated mass infall rate from the HVCs can be up to ~ 0.4 $M_{\odot}yr^{-1}$.

The work introduced in this thesis is driven from a straightforward sense that the HVC infall rates could be overestimated mainly from two reasons. (1) The hydrodynamic interaction between the inflowing cloud and the galactic disk is neglected in the estimation of the infall rate. (2) The infalling complexes will not always fully and progressively accumulate on the disk. Therefore, the "fuel supply rate" is newly defined as the true amount of HVC material that is donated to the galactic disk from the infalling HVCs when the hydrodynamic interaction between the cloud and the disk is considered. A total of 4 different infall cases are constructed with 11 HVC complexes of selection to show that the infall rate is overestimated compared to the true material supply rate. From the simulation results, it is shown that the fuel supply efficiency from HVCs infall can be as low as ~ 0.042 compared to the traditional maximum accretion scenario. The fuel supply efficiency is low for the reason that the HVC complexes selected for the simulations do not permeate further through the galactic disk as the densities of the selected HVC complexes are lower than the density of the gaseous disk. The fuel efficiency is increased with the density of the cloud as the hydrodynamical interaction between the disk and the complex is considered. Also identified is that the gas density of the cloud has an impact on the fuel supply efficiency and that the effect of the density is greater than that of the velocity of the approaching complex.

The simulations in this work do not include physical processes such as gravity, gravitational fields, cooling effects, and magnetic fields. On top of that, a uniform density profile is adopted for the interstellar medium (ISM), HVCs, and the galactic disk. All combined, the simulation in this study can be significantly improved for a better estimation of the true fuel supply rate. Nonetheless, the inefficiency of fuel supply through HVC material infusion that is suggested from the simulation results is valid.

One of the final goals of this study is to estimate the number of stars formed from HVC infall. Required for such work is a better estimation of the HVC fuel supply rate which can be provided by implementing a non-uniform density profile for the HVC complexes and the gaseous disk, adding gravity, magnetic field, and cooling, and further by investigating on the fraction of H_2 which is converted from the amount of HI supplied from the inflow of HVCs.

Contents

Acknowledgements . . . .

I Introduction 1

II Galactic Chemical Evolution (GCE) 3

2.1 Introduction 3

2.2 The Simple Model of Galactic Chemical Evolution 4

2.2.1 Formulation and Derivation 4

2.2.2 G-dwarf Problem: Counting the Number of Stars 8

2.2.3 Timescales in Chemical Evolution 9

2.3 Gas Flow and Chemical Evolution 10

III High-velocity Clouds (HVCs) 11

3.1 Introduction 11

3.2 Fundamental Equations 11

3.2.1 Deviation Velocity 11

3.2.2 Infall Rate 13

3.3 Origin of HVCs 13

3.3.1 Galactic Fountain 13

3.3.2 Tidal Stream 14

3.3.3 Accretion of Low-Metal Material 14

IV Estimating the Fuel Supply Rate on the Galactic Disk from HVC Infall 15

4.1 Introduction 15

4.2 Simulation Methods 15

4.2.1 Simulation Configurations 15

4.2.2 Parameters for HVC Infall 16

4.2.3 Fuel Efficiency and Timescale 18

4.3 Simulation Results 20

4.3.1 Proof of the Idea 20

4.3.2 HVC Infall Cases 23

4.3.3 Limitations 25

V Conclusion and Future work 26

A Derivation of the Initial Mass Function (IMF) 28

B Parameterization and Derivation of the Star Formation Rate (SFR) 30

C Stellar Yield 32

D Formulation and Derivation of the Simple Model of Chemical Evolution 34

E Further Complicated Galactic Chemical Evolution Models 36

F The Simple Kinematic Model: Distribution of HVC Locations and Velocities 40

G Physical Conditions for the Formation of a Galactic Fountain 42

References 44

List of Figures

1 The observed stellar metallicity distribution in the solar neighborhood (histogram) in comparison with the Simple Model prediction (line). The stellar yield, $y_Z = 0.010$ and the current time metallicity, $Z_1 = 0.017$. The data from Kotoneva et al.(2002) is used to reproduce the observational distribution [1]. Retrieved from the lecture notes of Professor Richard Mushotzky at the University of Maryland, copyrights reserved to their respective owners. 9

2 The all-sky map of High Velocity Clouds (HVCs) presented in galactic coordinates where the center is the Anti-Center [2,3]. The deviation velocity, $v_{\rm DEV}$ is displayed in colors where the scale is presented in the bar below the map. From definition, HVCs are the clouds with $|v_{\rm DEV}| > 90$ km/s. The clouds in gray are clouds with $|v_{\rm LSR}| > 90$ and $|v_{\rm DEV}| < 90$ km/s, therefore classified as intermediate velocity clouds (IVCs). 12

3 The interaction between Complex C and the galactic disk in terms of the total density (top) and the mass fraction of the HVC material only (bottom) for a period of 180 Myr while the interval between each panel is 20 Myr. The disk is the red layer at z=0 (top) and with the halo material existing in the background the complex is moving towards the disk with the velocity of 143.9 km/s and from the vertical distance of 12.04 kpc between the centers of the complex and disk. . 16

4 Schematic illustration of the infall parameters for a spherical HVC. D is the observed radial distance, Ω is the solid angle, and b is the galactic latitude. The area of detection, A, can be estimated from the distance and the solid angle which in turn is used for estimating the radius of the cloud from the following relation, $\Omega D^2 \sim A \sim R^2$. 18

5 The amount of HVC mass supplied to the galactic disk from Complex C inflow as a function of time. The step-function like shape represents the mass infusion in the traditional infall scheme where the mass of the infalling complex is completely infused into the gaseous disk. The simulated amount of fuel supplied from the HVC complex is described in a dotted line, whereas the dashed line illustrates the fuel supply process when the long-term physical effects are not compensated from the characteristic timescale, $2\tau_{char}$, since impact. 19

6 The first infall scenario, where five clouds with the same velocity but different distances are colliding with the galactic disk. The initial velocity of the inflowing clouds is 100 km/s and the distance is increased from 2 kpc up to 10 kpc with an increment of 2 kpc. The supply rate of HVC material is estimated at the times, $t = t_i + 2\tau_{char}$, for each inflowing HVC. 21

7 The second infall scenario, where the clouds are positioned at an initial distance of 4 kpc but the velocity among the HVCs varies from 40 km/s up to 120 km/s. The time evolution of the mass supplied to the gaseous disk (top panel) and the supply rate of HVC material estimated at the times, $t = t_i + 2\tau_{char}$, for each inflowing HVC (bottom panel). 22

8 Time evolution of the mass supplied into the galatic disk (top) and the rate of mass supply at the time, $t = t_i + 2\tau_{char}$, for each inflowing complex (bottom). A total of 4 different inflow scenarios are constructed for the infall of 11 different HVC complexes. Case 1 (red): complexes with maximum velocity and density. Case 2 (yellow): maximum velocity but intermediate density. Case 3 (green): intermediate velocity but maximum density. Case 4 (blue): both intermediate velocity and density. 24

I Introduction

Galactic Chemical Evolution (GCE) is the proportional buildup of helium and heavier elements within a galaxy over time. The enrichment in metals is driven by stellar nucleosynthesis over many generations of stars. To better understand our galaxy as an engine for global star formation, effectively utilized are galaxy-scale prediction models of the star formation processes. The earlier models are capable of describing the abundance distribution and the chemical enrichment history of closed systems such as the galactic bulge and globular clusters. However, when applied to the solar system that belongs to the Galactic arm region the number of metal-poor G-dwarfs are overpredicted compared to the observed number of such stars. Such discrepancy between the observed number of low-metal G-dwarfs and the number estimated by the analytical solution of the Simple Model is also known as the "G-dwarf problem". Previous studies on solving the G-dwarf problem includes allowing gas exchange at the boundaries of the system [4, 5], considering enriched infall [6], applying time-dependent initial mass functions [7], dealing with the stellar yield as a metal dependent variable [8], removing the instantaneous recycling approximation [9], taking into account inhomogeneous star formation [10], assuming prompt initial enrichment [11], and many more. Among the solutions, the infall of metal-poor gas is most supported and the progressive accretion of gas is also considered standard in the context of Λ-CDM cosmology [12].

Knowing that the estimation of the evolution of chemical abundances through GCE analytical models can be further improved by allowing the inflow of low-metal gas, the search has been carried on to identifying possible sources of such metal-poor gas. First detected through the 21 cm radio emission line by Muller et al. (1969) [13], High Velocity Clouds (HVCs) with the deviation velocities over 90 km/s are considered a suitable candidate for such low-metal inflowing material assuming that the HVCs are not only a local phenomenon but a universal entity which also can be observed in other galaxies. The estimated maximum accretion rate of the approaching HVCs on our galaxy can be up to ~ 0.4 $M_{\odot}yr^{-1}$ [14] which is comparable to the accretion rate required by chemical evolution models that is ~ 0.45 $M_{\odot}yr^{-1}$ [15]. However, the maximum accretion rate which is also known as the traditional "infall rate" does not consider the kinematic consequences from the hydrodynamic interactions between the inflowing HVCs and the galactic disk. Therefore, newly defined is the "fuel supply rate" which describes the true amount of material that is supplied to the galactic disk from the inflow of HVCs [16].

The ultimate objective is to improve the GCE model prediction on the evolution history of chemical abundances by introducing the number of stars formed through the extra material provided by HVC infall. Addressed in this thesis is the estimation of the true amount of HVC material that is supplied to the system from HVC infall. While detailed investigation on the relationship between dust and HI-H_2 conversion is also required, the estimation of HVC fuel supply itself can serve as a groundwork for later estimating the number of stars formed from the fuel provided by HVCs with further improved quantitative analyses and simulations.

In the following Chapter 2, presented is how the evolution of gas and metals can be numer-

ically estimated through analytical GCE models. In Chapter 3, the basic properties and the traditional infall rate of the HVCs are introduced. In Chapter 4, described is the estimated amount of true fuel supply and the efficiency from the simulation results and how it can vary from the traditional infall rate. Finally, in Chapter 5 the conclusion and a brief description on the future work are given.

II Galactic Chemical Evolution (GCE)

2.1 Introduction

The word Galaxy is originated from the ancient Greek myth describing that our Milky Way was created from a lost drop of milk when goddess Hera was breastfeeding Heracles, where the word milk is called 'gala' in Greek. Then it was first observed by Galileo around 1610, that our Milky Way consists of also stars and is not simply made of some kind of celestial fluid. After that, the development of various telescopes and insightful studies of our sky have led to the point where we describe our galaxy as a rotating spiral in the shape of a flattened disk ($\sim$ 200 pc thick according to the definition of thin disk) which extends up to $\sim$ 25 - 30 kpc from the center of the bulge. Through a number of observations and a large amount of spectroscopic data not only the physical structure of our Milky Way has been revealed but the fact that different stars with different ages carry different chemical compositions and that the metallicity of those stars decreases as the age of the star increases have also been discovered. Such relationship between the age and the metallicity of different stars is considered as evidence of progressive chemical enrichment in our galactic system and it is also the motive to the study of reconstructing the history of chemical enrichment in our galaxy.

The study of Galactic Chemical Evolution (GCE) focuses on tracking the chemical composition which is a result of the creation and destruction of stars and discovering how they can be distributed in galaxies. Doing so can provide a framework for one to (1) chronologically order the events in a galaxy by determining when a stellar source contributed to the abundance of a specific element, (2) numerically express the effect of stellar nucleosynthesis on the evolution of a galaxy in terms of stellar yield from the abundance dispersion and ratios, and (3) infer the mechanism of how a galactic system could have been formed by constraining the star formation rate (SFR) and trailing gas movements.

It is considered that the production and evolution of chemical elements in a galaxy-scale large body are primarily driven by stellar nucleosynthesis throughout countless generations of stars. Chemical elements are produced inside the stars then ejected back into the interstellar medium (ISM) where new stars are again created and such cycle is to be repeated. Accordingly, the most evident way to unveil the history of chemical enrichment and distribution in a galaxy is to search for and investigate the stars that have a very long lifetime because such stars would act as "fossils" which enclose information about the chemical abundances at approximately the time they were born. However, a job of collecting a good amount of stars enough to explain the complete evolution history of the chemical abundance in a galaxy is nearly impossible to accomplish due to observational limitations. Instead of collecting fossils, an alternative method is to build an analytical model from the basic knowledge of physics and our galaxy.

2.2 The Simple Model of Galactic Chemical Evolution

In fact, chemical evolution models of many kinds have been actively constructed and developed throughout the past $\sim$ 60 years, providing such a useful framework for one to estimate the abundances in the gas (ISM) and stars of a galaxy. While there are so many studies on the subject of chemical evolution models that are worth mentioning, I think it will be most reasonable to begin with introducing the formulation and derivation of the simple model which can be used as a groundwork for further complicated models.

2.2.1 Formulation and Derivation

Motivated from the idea that the metal abundance of the stars and gas in a system must evolve in time, one of the earliest efforts on analytically predicting the chemical enrichment of a galaxy driven by the synthesis and loss of stellar mass is named the "Simple model of galactic chemical evolution" [17]. It is called the "simple" model because the process of manipulating chemical enrichment in the model is built upon strong basic assumptions such as listed.

(1) The system at the initial state contains no stars; only pure gas with primordial abundances

(2) Instantaneous recycling and mixing of metals; well-mixed homogeneous system

(3) The galaxy is a closed system with a fixed total mass; inflow or outflow of material is not allowed

(4) Constant stellar yield; the fraction of stellar ejecta into the gas is fixed

Additional core ingredients mandatory for building an analytical GCE model are the initial mass function (IMF) and the star formation rate (SFR) which can be combined to define the stellar birthrate function expressed as the product of the IMF and the SFR. The IMF, $\varphi(m)$, is commonly estimated in the following form,

$$\varphi(m) = Am^{-(1+x)} \tag{2.1}$$

where x is called the slope of the function which can have different values for different mass ranges and A is a normalization constant that can be obtained from normalizing $\varphi(m)$ as following.

$$\int_0^\infty m\varphi(m)\mathrm{d}m = 1 \tag{2.2}$$

Since the process of star formation is barely known and yet a mystery, the SFR, $\psi(t)$, as a funtion of time is usually described proportional to some power, k, of the volume gas density, ρ_{gas},

$$\psi(t) \propto \rho_{\rm gas}^{k} \tag{2.3}$$

following the original parametrization suggested by Schmidt (1959) [17].

Now we turn to the stellar birthrate function, $B\,(m,t)$, which is defined as the number of stars born in the time interval t, $t+\mathrm{d}t$ and the mass interval m, $m+\mathrm{d}m$ by combining the two independent functions of the SFR and the IMF as,

$$B(m,t) = \varphi(m)\psi(t)\mathrm{d}m\mathrm{d}t \tag{2.4}$$

However, it is a well-known problem that the SFR and the IMF are indeterminate when separated, meaning that either of them should be pre-assumed in order to have the other one to be derived since we have information only for the mass of the stellar component and the gas component at the current time.

Now that we have the ingredients for constructing an analytical chemical evolution model, we start by defining the total mass, $M_{\rm tot}$, as,

$$M_{\rm tot} = M_{\rm gas} + M_{\rm star} \tag{2.5}$$

where $M_{\rm gas}$ is the total mass of gas in the system and $M_{\rm star}$ is the mass of stars. $M_{\rm star}$ here consists of both the mass of living stars $M_{\rm S}$ and stellar remnants $M_{\rm R}$ which could be neutron stars (NS), white dwarfs (WD), and black holes (BH). The total dynamical mass of a galaxy $M_{\rm galaxy}$, includes both the baryonic matter and the non-baryonic dark matter $M_{\rm dark}$ so that $M_{\rm galaxy} = M_{\rm gas} + M_{\rm S} + M_{\rm R} + M_{\rm dark}$. However, in the simple model $M_{\rm dark}$ is not considered and therefore the total mass in the system is described in the mass of only gas and stars.

The fractional mass of gas, μ, is defined such as,

$$\mu = \frac{M_{\rm gas}}{M_{\rm tot}} \tag{2.6}$$

so that we can express the mass of the stars, $M_{\rm star}$, as following.

$$M_{\rm star} = (1-\mu)M_{\rm tot} \tag{2.7}$$

The metallicity, Z, is defined as,

$$Z = \frac{M_Z}{M_{\rm gas}} \tag{2.8}$$

where M_Z is the total mass of metals of the galaxy (i.e. the elements that are heavier than helium).

From Assumption (1) we know that

$$M_{\rm gas}(0) = M_{\rm tot} \tag{2.9}$$

and that

$$Z(0) = 0 \tag{2.10}$$

as the system at the initial state contains no stars but only gas with primordial abundances.

The evolution of the gas in such system is estimated as,

$$\frac{\mathrm{d}M_{\mathrm{gas}}}{\mathrm{d}t} = -\psi(t) + E(t) \tag{2.11}$$

where $E(t)$ is the rate of material being returned into the ISM from dying stars which in turn is estimated as,

$$E(t) = \int_{m(t)}^{\infty} (m - M_{\mathrm{R}})\psi(t - \tau_m)\varphi(m)\mathrm{d}m \tag{2.12}$$

where $m(t)$ is the mass that is created at the time $t = 0$ which is to die at the time t and M_{R} is the mass of the remnant. Accordingly, $m - M_{\mathrm{R}}$ will be the mass ejected from a star with an initial mass of m and lifetime of τ_m. However, in the simple model, the lifetime of the stars can be neglected by adopting Assumption (2), namely the instantaneous recycling approximation (IRA) whereas stars with mass < 1 $\mathrm{M}_{\odot}$ does not die while the death of all other stars occurs instantaneously. Adopting such approximation allows one to define the fraction of mass from a stellar generation that is returned into the gas, R, such as following.

$$R = \int_{1}^{\infty} (m - M_{\mathrm{R}})\varphi(m)\mathrm{d}m \tag{2.13}$$

R is to be a constant typically found at $0.20 - 0.50$ depending on the normalization of the IMF which is further discussed in Appendix A.

The yield is defined as the ratio between the total mass of synthesized metals and the ejected mass of those metals from the stars with a mass > 1 $\mathrm{M}_{\odot}$. Along with the SFR and IMF, the yield plays an important role in estimating the time evolution of chemical enrichment as it determines the amount of newly produced metals that is dumped back into the ISM. The mathematical definition for such quantity is also based on the approximation of instantaneous death and recycling of stars, which is given as,

$$y_Z = \frac{1}{1 - R}\int_{1}^{\infty} m p_{Zm}\varphi(m)\mathrm{d}m \tag{2.14}$$

where m is the initial stellar mass and $p_{Zm} = (M_{ejected})_Z/m$ is the mass fraction of the newly synthesized and then ejected metals from a star with mass m.

Now Equation (2.12) can be expressed as,

$$E(t) = \psi(t)R \tag{2.15}$$

and Equation (2.11) as following.

$$\frac{\mathrm{d}M_{\mathrm{gas}}}{\mathrm{d}t} = -\psi(t)(1 - R) \tag{2.16}$$

In the perspective of chemical evolution, one of the objectives is to express the evolution of metals, Z, in terms of the mass of the stars and gas.

Similar to Equation (2.11), we estimate the evolution of the mass of heavy elements as,

$$\frac{\mathrm{d}ZM_{\mathrm{gas}}}{\mathrm{d}t} = -Z\psi(t) + E_Z(t) \tag{2.17}$$

where the later term on the right side of Equation (2.17) is given as,

$$E_Z(t) = \int_{m(t)}^{\infty} [(m - M_{\mathrm{R}})Z(t - \tau_m) + mp_{Zm}]\psi(t - \tau_m)\varphi(m)\mathrm{d}m \tag{2.18}$$

so that the ejected mass from primordial materials which does not undergo nucleosynthesis is considered in the first term inside the square brackets and the second term is the mass ejected from newly synthesized metals. Again with the IRA, Equation (2.18) is re-written as,

$$E_Z(t) = \psi(t)RZ(t) + y_Z(1 - R)\psi(t) \tag{2.19}$$

which can be substituted into Equation (2.17) so that we obtain the expression for the change in metal mass as following.

$$\frac{\mathrm{d}ZM_{\mathrm{gas}}}{\mathrm{d}t} = -Z\psi(t) + \psi(t)RZ(t) + y_Z(1 - R)\psi(t) \tag{2.20}$$

From Equation (2.16) and the product rule of derivation, Equation (2.20) is re-arranged as,

$$M_{\mathrm{gas}}\frac{\mathrm{d}Z}{\mathrm{d}M_{\mathrm{gas}}} = -y_Z \tag{2.21}$$

which can finally be integrated from $Z(0)$ to $Z(t)$ and from $M_{\mathrm{gas}}(0)$ to $M_{\mathrm{gas}}(t)$ to obtain the analytical solution as following.

$$Z = y_Z \ln(\frac{1}{\mu}) \tag{2.22}$$

A different approach on deriving the simple model is also introduced in Appendix D. Additionally, the derivation of further complicated models that consider gas flow through biased galactic winds, galactic fountains from SNe, and radial flows is provided in Appendix E.

The observed metallicity can be compared with the metallicity estimated from the simple model solution stated in Equation (2.22), assuming that the yield is location independent. The observed result in spiral galaxies shows that the gas fraction in the galactic disk increases towards the edge of the disk and therefore the metallicity, Z, decreases in the following direction. But in reality, it is observed that the decrease in metallicity is steeper at the direction towards the edge of the disk compared to the simple model estimation. It is introduced in this section how a simple analytical model can be constructed to estimate the time evolution of metallicity in a galaxy. The simple model can be fairly reliable when describing the chemical evolution of a system that is nearly closed such as the galactic bulge. However due to the basic assumptions such as considering a system as a closed box, using a constant initial mass function and many more, the model is not capable of illustrating the evolution of open systems like the galactic disk.

2.2.2 G-dwarf Problem: Counting the Number of Stars

It was introduced in the previous section, how an analytical model could be constructed in order to estimate the time evolution of metallicity in a galaxy. Using the same model one can successfully estimate the fraction of stars to the gas which in turn allows one to predict how the fraction of stars would vary depending on the metallicity.

We re-write the simple model analytical solution given in Equation (2.22) in terms of the mass of stars and the mass of gas in the system such as,

$$Z = -y_Z \ln\left(\frac{M_{\rm gas}(0) - M_{\rm stars}(t)}{M_{\rm gas}(0)}\right) \tag{2.23}$$

and the terms can be rearranged as following.

$$\frac{M_{\rm stars}(t)}{M_{\rm gas}(0)} = 1 - e^{-Z(t)/y_Z} \tag{2.24}$$

As it is easier to obtain the present time observation data of our galaxy than to predict the mass of the gas at the initial state, we can also describe the metallicity at the present time, t_p, such as,

$$\frac{M_{\rm stars}(t)}{M_{\rm stars}(t_p)} = \frac{1 - e^{-Z(t)/y_Z}}{1 - e^{-Z(t_p)/y_Z}} \tag{2.25}$$

where, $M_{\rm stars}(t_p)$ and $Z(t_p)$ are the mass in the stars and the metallicity, respectively, both at the current time, t_p.

Assuming that the number of stars, $N(Z)$, with a metallicity ,$\leq Z$, is proportionial to the total mass of such stars so that $N(Z) \propto M_{\rm stars}(t)$, we obtain,

$$\frac{N(Z)}{N(t_p)} = \frac{M_{\rm stars}(t)}{M_{\rm stars}(t_p)} \tag{2.26}$$

where $N(t_p)$ is the number of stars at the present time, t_p. The Equation (2.26) can be substituted into Equation (2.25) so that we have,

$$\frac{N(Z)}{N(t_p)} = \frac{1 - e^{-Z(t)/y_Z}}{1 - e^{-Z(t_p)/y_Z}} \tag{2.27}$$

as the relation between the number of stars and the fraction of heavy elements (i.e. metallicity).

However, it was found that the distribution of the number of stars as a function of metallicity predicted from the Simple Model did not match the observation data of the stars in our solar neighborhood. Compared to the observations, the number of low-metal stars at [Fe/H] ≤ -1.0 dex was over-predicted in the GCE simple model. Such discrepancy is also known as the "G-dwarf problem" first discovered by van den Bergh (1962) and Schmidt (1963) [18,19]. Described in Figure 1 is the G-dwarf problem where the histogram represents the number of stars as a function of [Fe/H] and the curve is the simple model prediction.

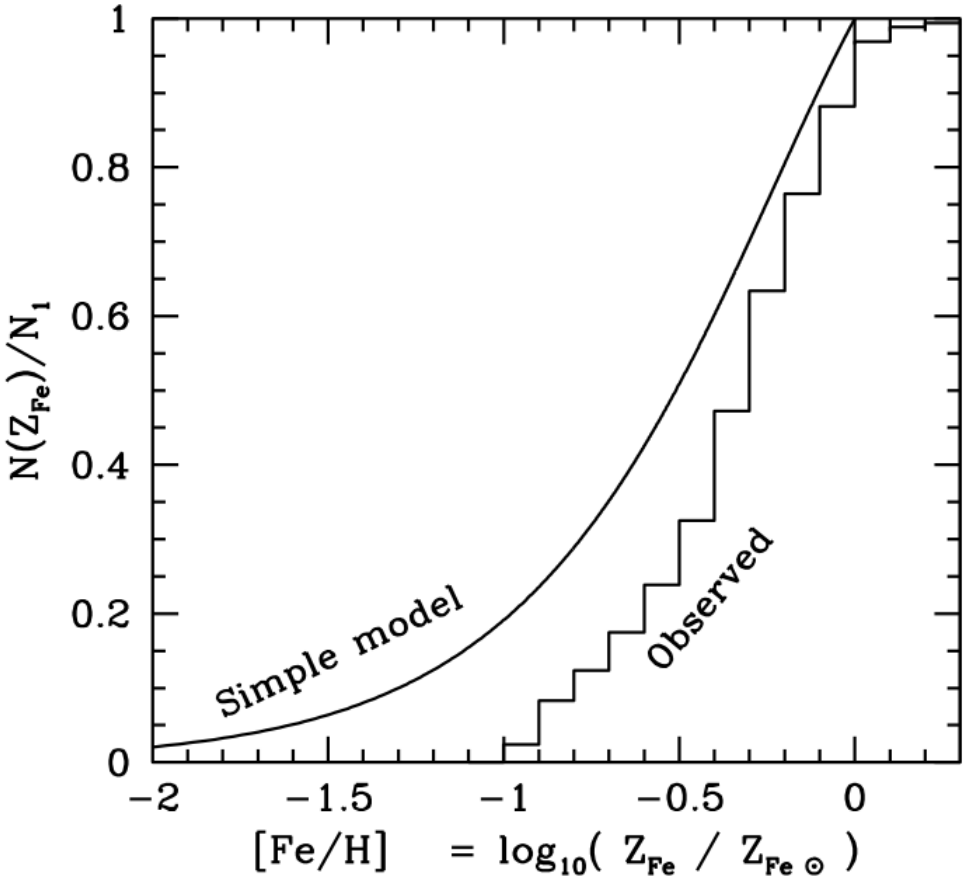

Figure 1: The observed stellar metallicity distribution in the solar neighborhood (histogram) in comparison with the Simple Model prediction (line). The stellar yield, $y_Z = 0.010$ and the current time metallicity, $Z_1 = 0.017$. The data from Kotoneva et al.(2002) is used to reproduce the observational distribution [1]. Retrieved from the lecture notes of Professor Richard Mushotzky at the University of Maryland, copyrights reserved to their respective owners.

2.2.3 Timescales in Chemical Evolution

As in many other theoretical models that describe dynamical processes, certain timescales can be examined to verify the reliability of the models. In GCE models, often defined is the star formation timescale which is equivalent to the time required for gas depletion. The star formation timescale, $\tau_{\rm SF}$, is defined as,

$$\tau_{\rm SF} = \frac{M_{\rm gas}}{|{\rm d}M_{\rm gas}/{\rm d}t|} = \frac{M_{\rm gas}}{(1-R)\psi} \tag{2.28}$$

Another timescale that is often used in GCE is the chemical enrichment timescale which is defined as,

$$\tau_Z = \frac{Z}{|{\rm d}Z/{\rm d}t|} = \frac{Z M_{\rm gas}}{y_Z(1-R)\psi} \tag{2.29}$$

For the simple model of the solar neighborhood, under the assumption that the surface mass density is 10 $\rm M_\odot pc^{-2}$ and the SFR at current time is 10 $\rm M_\odot pc^{-2} Gyr^{-1}$, the star formation

timescale, $\tau_{\rm SF}$, is estimated as ~ 1 Gyr. With an additional assumption that the stellar yield and the current time metallicity are comparable, the chemical enrichment timescale, τ_Z, is estimated as ~ 1 Gyr. It is unlikely that the solar neighborhood is at its end-stage and the gas is to be consumed only after ~ 1 Gyr. It is also evident from the age-metallicity relation from observations that the metallicity increases slower in time compared to the estimated enrichment timescale. Hence, it is shown from the timescales in Equation (2.28) and Equation (2.29) that the basic assumptions for the simple model do not hold in open systems such as the solar neighborhood.

2.3 Gas Flow and Chemical Evolution

In the context of GCE and analytical chemical evolution models, the effect of gas flows is one of the most important elements for reproducing a galaxy and understanding the formation process. As a summary, provided below are some useful and insightful theorems based on the study of the effects of gas flows on the GCE models by Edmunds [20].

(T1) The G-dwarf problem can be solved with low-metal gas infall. The problem cannot be solved by gas outflow.

(T2) In an outflow dominated system where the inflowing gas is metal-poor, the effective yield is lower than the Simple Model prediction of yield.

(T3) In a system with primordial and unenriched gas inflow, the effective yield is lower than the Simple Model prediction of yield.

(T4) With only outflow and no inflow, the mass-weighted mean stellar metal abundance is lower than the Simple Model prediction of metallicity.

(T5) Without any gas exchange from outside the box, the gas metallicity gradient is steeper than the stellar metallicity gradient.

(T6) The chemical enrichment of gas with radial gas flow is independent of the distribution of gas, provided that the star formation is proportional to the first power of the gas density.

(T7) The SFR is the first power of the gas density and a function of time in a system which does not allow gas accretion.

(T8) The ratio between the primary and the secondary element is independent of radial gas flows, only in a system without gas accretion.

III High-velocity Clouds (HVCs)

3.1 Introduction

It is observed that the dense interstellar medium (ISM) is mostly filled in the Galactic plane and rotating around the Galactic center (GC). Energetic events and processes can allow a bulk motion of gas in the ISM at an abnormal velocity which could deviate from the Galactic circular rotation up to $\sim$ 300 km/s. Through the 21 cm radio emission line, such high-velocity clouds (HVCs) were first discovered by Muller, Ooort, and Raimond (1963). Letters of the alphabet were assigned to the observed HVC complexes as their names in a way that a complex would be distinguishable from another. For example, the first discovered three were given the letters A, B, and C. Complexes M, H, and K were given the letters after the name of their discoverers who are Mathewson, Hulsbosch, and Kerr, respectively. AC is located near the Anti-Center and GCN is close to the Galactic center. Complexes WA, WB, WC, WD, WE were named after their discoverers Wannier, Wrixon and Wilson (1972) and also after Wakker and van Woerder (1991) who first catalogued them. The size of an HVC complex is typically in the range from a few kpc up to 15 kpc across and the HI mass is $10^5 \sim 10^6$ $M_\odot$. Generally agreed is that the complexes predominantly exist at a distance $\leq$ 10 kpc, while further constraints on the exact distances are required [14,21,22]. Estimated is that the HVCs with N(HI)$> 7 \times 10^{17}$cm^{-2} covers $\sim$ 30% of the sky and those with N(HI)$> 10^{18}$cm^{-2} covers about $\sim$ 10% [23].

From the lists of Hulsbosch and Wakker(1988) and Morras et al. (2000) an all-sky map of the HVCs is visualized in Figure 2. The colors describe the deviation velocity, $v_{\rm DEV}$, and the positive and negative sign shows the direction of the clouds. Following Wakker's definition of HVCs, a cloud with a deviation velocity, $|v_{\rm DEV}| > 90$ km/s is classified as an HVC. Note that the grey colored clouds have the local standard of rest velocity, $|v_{\rm LSR}| > 90$ km/s but $|v_{\rm DEV}| < 90$ km/s and therefore not classified as HVCs but intermediate velocity clouds (IVCs). It is also identified in the figure that the majority of HVCs show negative local standard of rest velocities $v_{\rm LSR}$ at $0^\circ < l < 180^\circ$ and positive $v_{\rm LSR}$ at $180^\circ < l < 360^\circ$. This is because the local standard of rest (LSR) is moving towards $l = 90^\circ$, $b = 0^\circ$ at the velocity of 220 km/s and the HVCs not participating in Galactic rotation but moving along such direction will show negative velocities. Clouds with positive velocities would be found near $l = 90^\circ$ and those with negative velocities near $l = 270^\circ$ assuming that the velocity spread is larger than $\pm$300 km/s. This can be also explained through the simple kinematic model of the distribution of cloud locations and velocities that is provided in Appendix F.

3.2 Fundamental Equations

3.2.1 Deviation Velocity

Defined by Wakker (1991) the deviation velocity, $v_{\rm DEV}$, describes the deviation between the observed LSR velocity and the maximum velocity of galactic rotation. Depending on the direction

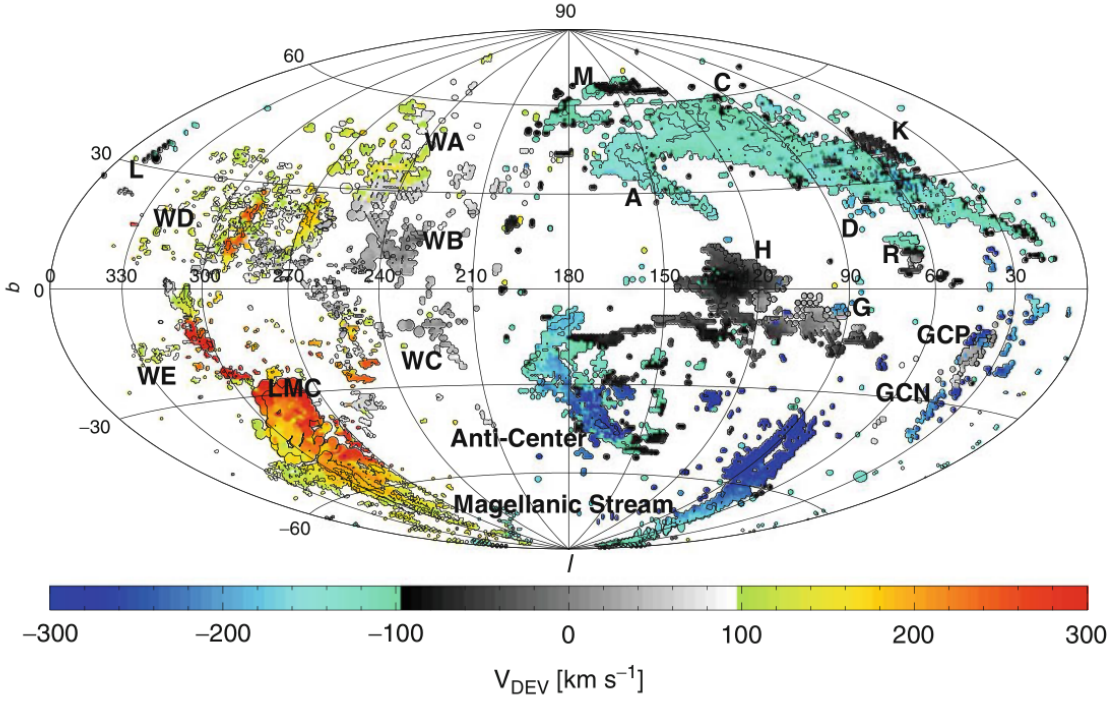

Figure 2: The all-sky map of High Velocity Clouds (HVCs) presented in galactic coordinates where the center is the Anti-Center [2, 3]. The deviation velocity, $v_{\rm DEV}$ is displayed in colors where the scale is presented in the bar below the map. From definition, HVCs are the clouds with $|v_{\rm DEV}| > 90$ km/s. The clouds in gray are clouds with $|v_{\rm LSR}| > 90$ and $|v_{\rm DEV}| < 90$ km/s, therefore classified as intermediate velocity clouds (IVCs).

of LSR velocity the deviation velocity can be calculated as,

$$v_{\rm DEV} = v_{\rm LSR} - v_{g,\rm min} \qquad \text{where } v_{\rm LSR} < 0 \tag{3.30}$$

$$v_{\rm DEV} = v_{\rm LSR} - v_{g,\rm max} \qquad \text{where } v_{\rm LSR} > 0 \tag{3.31}$$

where $v_{g,\rm min}$ is the minimum velocity possible in the disk that is rotating in the same direction of $v_{\rm LSR}$, $v_{g,\rm max}$ is the maximum velocity possible.

v_g is estimated from the vertical distance to the galactic plane, z, and the galactocentric radius, R depending on the location based on the galactic longitude l and latitude b such as,

$$v_g(l,b,d) = \left[\frac{R_0}{R}v(R) - v(R_0))\sin(l)\cos(b)\right] \tag{3.32}$$

$$R(l,b,d) = R_0\sqrt{\cos^2(b)\frac{d}{R_0}^2 - 2\cos(b)\cos(l)\frac{d}{R_0} + 1} \tag{3.33}$$

$$z(l,b,d) = d\sin(\mathrm{b}) \tag{3.34}$$

where d is the line of sight distance, R_0 is the distance of the Sun from the Galactic Center (GC), and $v(R)$ is the galactic rotation curve. R_0 is measured as ~ 7.9 kpc and $v(R) = 220$ km/s at $R > 0.5$ kpc.

3.2.2 Infall Rate

Estimated from the physical configuration of the HVCs including distance, mass, and velocity the mass infall rate is traditionally expressed as,

$$\dot{M} = \sum \frac{M_i v_i}{D_i} \tag{3.35}$$

where M_i is the mass of a high-velocity cloud, v_i is the observed radial velocity, and D_i is the distance [14, 21]. Therefore, the total infall rate of HVC complexes is the sum of the infall rate of each inflowing HVC. Estimating the rate of gas infall using Equation (3.35), one can benefit from the simplicity of directly handling the observed mass, velocity, and distance. However, the actual path and motion, exact distance, the distribution, and impact position of the HVCs cannot be determined from observations.

For such reason, the infall rate is parameterized in the chemical evolution models. Notable parameterizations of the mass infall rate from extragalactic material include the exponentially decreasing function of time [24], the increasing function of the galactocentric radius [25], the exponentially decreasing function of both the time and the galactocentric radius [26], and the two-infall model depending on the thickness of the disk [27].

3.3 Origin of HVCs

It is revealed from observations, including the Milky Way that there are galaxies with a thick layer of HI and a population of HVCs which can extend to a few tens of kpc from the galactic plane. From the distribution of HI in many galaxies, further discovered was the accretion of gas from intergalactic clouds and/or dwarf galaxies. While there are various theories on the source of HVCs since its discovery, such observations support the idea that the HVCs come from multiple origins. A few of the most frequently mentioned theories on the origin of HVCs are discussed in the following subsections.

3.3.1 Galactic Fountain

A concept of a galactic scale hot gas flow in the ISM was introduced by Shapiro and Field (1976) [28]. The source of a gas outflow of such scale includes radiation, stellar winds, and successive SNe within the galactic plane which will heat up the gas in the disk. Then the cooling process will promote the condensation of the ejected gas into atomic hydrogen clouds. Such clouds will eventually fall down towards the galactic disk at anomalous velocities to form what is called a galactic fountain. Such idea of a galactic scale gas flow has been revisited and galactic fountain models have been developed ever since. The 2-D models by Houck & Bregman (1990) and Rosen et al. (1993) [29, 30], the 3-D models by de Avillez (2000), Joung & Mac Low (2006) and Kwak et al. (2009) [31–33], and the analytic models by Bregman (1980) and Kahn (1981) are noteworthy fountain models [34, 35]. The physical conditions required for

the galactic fountain formation can be derived from the cooling timescale and the dynamical timescale [35, 36]. The derivation is further introduced in Appendix G.

3.3.2 Tidal Stream

Some HVCs are evidently in connection with the Magellanic Stream which is known as gas stripped out from the Small Magellanic Cloud (SMC). The metallicity is measured as $Z/Z_\odot \sim 0.3$ for the Magellanic Stream, which is consistent with the abundances in stars and gas of the SMC [37–39]. Such removal of gas from dwarf galaxies is caused from either ram pressure or tidal stripping. The gas at the outer region of the SMC is pulled out from the tidal force of the LMC combined with the tidal force of the Milky Way [40–42]. The leading arm of the stream is predicted and also observed to be spread around $l = 320°$, $b = -22°$. Moving through a coronal gas with a density of 10^{-4} cm^{-3} and a velocity of ~ 300 km/s, an HVC can experience ram pressure [34, 43, 44]. Observed in the case of dwarfs that are passing the Milky Way from a distance of about ~ 200 kpc, is that such dwarfs contain only a small amount of remaining gas. The gas is considered to be stripped by ram pressure as such pressure is comparable to the gravitational force [45].

3.3.3 Accretion of Low-Metal Material

Directly from the observations, there is evidence that the accretion of low-metallicity gas is an ongoing process. Complex C is seen approaching to the galactic disk at a vertical velocity of $50 - 150$ km/s from a distance of ~ 10 kpc. The metallicity of the complex is $Z/Z_\odot \sim 0.15$ and the (N/O) ratio is ~ 0.2 times solar implying that it is composed of extragalactic material [46,47].

IV Estimating the Fuel Supply Rate on the Galactic Disk from HVC Infall

4.1 Introduction

It was introduced in Section 3.2.2 that the traditional infall rate is estimated from Equation (3.35). The simplicity that allows one to directly use the observed mass, velocity, and distance of HVC complexes as an input to a GCE model is a great advantage. However, the limitations are clear since the observed distance, D_i, does not represent the distance from the location of the HVC to where the cloud will collide with the disk. The observed radial velocity, v_i, will not be the same with the radial velocity due to gravitational acceleration/deceleration. Above all, the infall rate represents a simple mass flow rate which does not consider the kinematic consequences which occur from the hydrodynamic interaction between the galactic disk and the inflowing gas. In other words, the prediction of the "infall rate" is based upon the traditional assumption of complete and steady accretion of the HVC material up until to the "time to impact ($= v_i/D_i$)".

In the following work, qualitatively presented is how the "fuel supply rate" can result in different values compared to the infall rate depending on the physical configuration (i.e. different combinations of density, radius, velocity, and distance) of the inflowing HVCs. Furthermore, a total of four different infall scenarios including the maximum and minimum infall cases are constructed with 11 different HVC complexes. From the numerical simulation results of the four infall scenarios, described is to what degree the rate of material supply could differ from the traditionally estimated infall rate depending on the velocity, mass, and distance of each inflowing HVC complex.

4.2 Simulation Methods

4.2.1 Simulation Configurations

The FLASH 2.5 code developed at the University of Chicago Flash Center is used for the simulations [48]. It serves as an adaptive-mesh, modular, and parallel simulation code that can deal with general compressible flow problems. The Message-Passing Interface (MPI) library is used for parallelization and the Adaptive Mesh Refinement (AMR) is managed from the PARAMESH library. The configuration of the computation domain is a 2-D cylindrical geometry that can be extended up to 10 kpc wide (r-direction) and 40 kpc long (z-direction) depending on the size and distance of the approaching complex. The refinement level is gradually increased to the maximum level that can be translated to a spatial resolution of $(9.7\ \mathrm{pc})^2$ for each cell as the material in the simulated inflowing HVC complex begins to interact with the gas in the galactic disk. The outflow of gas is allowed at the boundaries except at r = 0 (i.e. the vertical axis) where the material is reflected. The gaseous galactic disk is 250 pc thick and the HI volume number density is 0.1 cm^{-3} which is denser by three orders of magnitude compared to the ISM [49, 50].

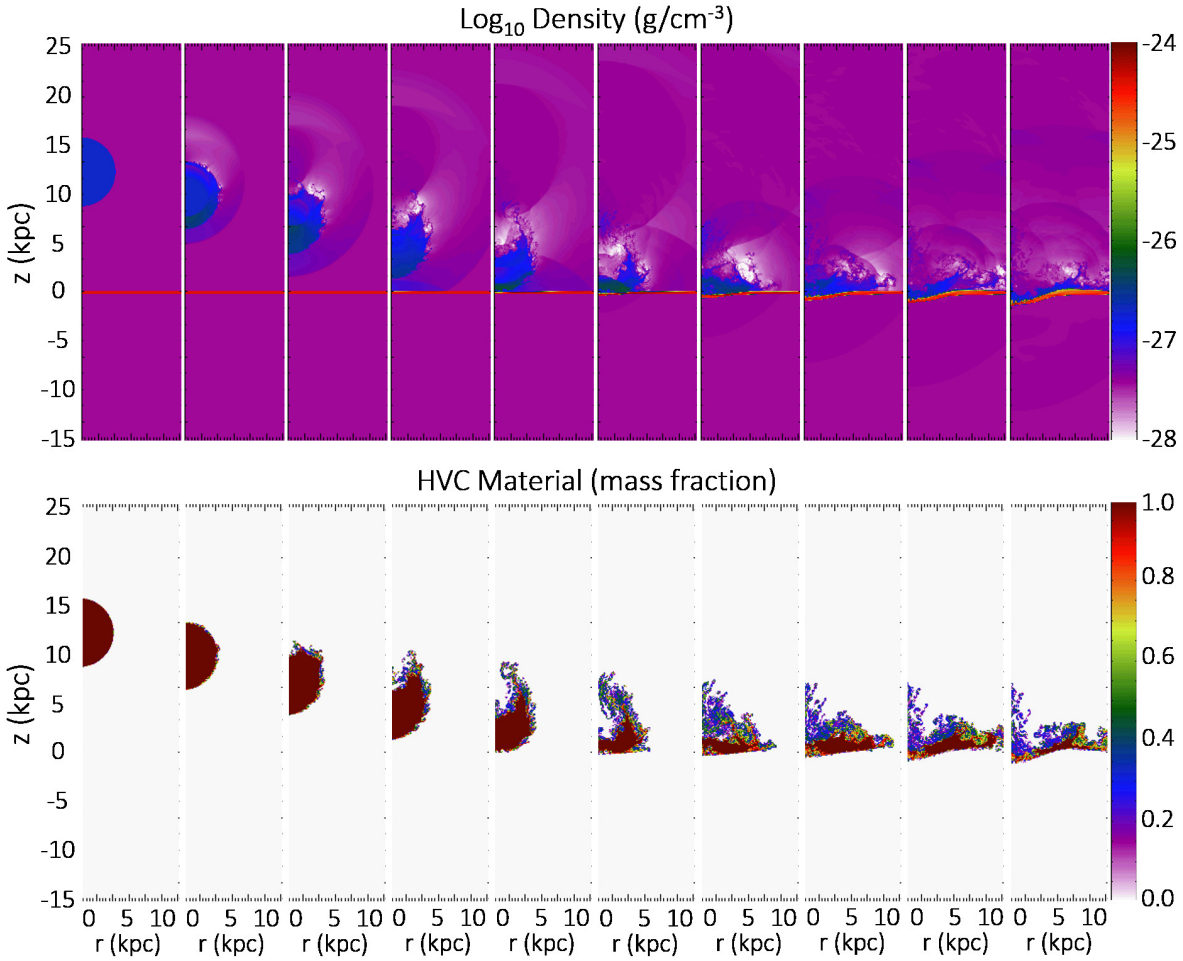

Figure 3: The interaction between Complex C and the galactic disk in terms of the total density (top) and the mass fraction of the HVC material only (bottom) for a period of 180 Myr while the interval between each panel is 20 Myr. The disk is the red layer at z=0 (top) and with the halo material existing in the background the complex is moving towards the disk with the velocity of 143.9 km/s and from the vertical distance of 12.04 kpc between the centers of the complex and disk.

4.2.2 Parameters for HVC Infall

A total of 11 different HVC complexes are carefully selected from Wakker's HVC catalogue [51]. The mass ($M(R, \mathrm{n})$), distance (D), latitude (b), and deviation velocity (v_{DEV}) are adopted mainly from the same catalogue but the data set is also supplemented with the observation results mentioned in other studies [22, 52–55]. From the parameters provided in Table 1, the vertical velocity (v_z) and distance (D_z) are determined.

How the velocity and radius (size) can be estimated for each complex from the observed solid angle (Ω), distance, and the galactic latitude (b) is illustrated in Figure 4. For each inflowing complex, estimated are two different vertical velocities, v_z; (1) by assuming a purely radial

Table 4.1: HVC Infall Parameters

Name of the Complex	Ω^a [$^{\circ 2}$]	b^b [$^\circ$]	v^c_{dev} [$km\ s^{-1}$]	D^d [kpc]	M^e [$10^6 M_\odot$]
A	288	+40	141	8.0	1.0
ACHV	397	-30	100	10.0	1.0
ACVHV	338	-30	221	10.0	1.0
C	1546	+58	122	10.0	5.0
GCN	130	-31	243	20.0	0.22
M	174	+62	95	4.0	1.0
GCP(Smith Cloud)	58	+13.4	73*	12.4	1.0
WA	102	+32	126	8.0	0.13
WB	289	+32	52	8.0	0.70
WD	253	+32	106	4.4	1.1
WE	51	-20	106	9.4	0.12

[a]Solid angle, [b]galactic latitude, [c]deviation velocity, [d]distance, and [e]mass. The *vertical velocity (i.e., v_z) of the Smith cloud is 73 km/s for the intermediate case and 99 km/s for the extreme case [53].

observed velocity,

$$v_z = v_{\rm DEV} \cdot \sin(b) \tag{4.36}$$

which we define as the intermediate velocity or (2) by assuming a vertical space velocity so that,

$$v_z = v_{\rm DEV} / \sin(b) \tag{4.37}$$

which we define as the extreme vertical velocity. Assuming that the infalling HVC complex follows a uniform density profile and the shape of the complex is a perfect sphere, the radius of the complex, R, can be estimated from the relation,

$$\Omega D^2 \ \sim \ A \ \sim \ R^2 \tag{4.38}$$

where Ω is the solid angle given from observation, D is the observed radial distance, and A is the area of detection. However, the true size of an HVC complex cannot be easily determined due to observational limitations. Therefore, an extreme (i.e. minimum radius) case is also considered by simply reducing the intermediate radius into half. Then the relation described in Equation (4.38) is now $\Omega D^2 \ \sim \ A \ \sim \ 2R^2$ so that we obtain a denser and smaller complex. The mass of each complex is remained constant in both cases where the HI volume number density of the HVC complexes can vary from 1.14×10^{-5} cm^{-3} (for the intermediate density of Complex GCN) to 2.03×10^{-2} cm^{-3} (for the extreme minimum radius of Complex WD). Given two different velocities from Equation (4.36, 4.37) and two different radii (one as the extreme and

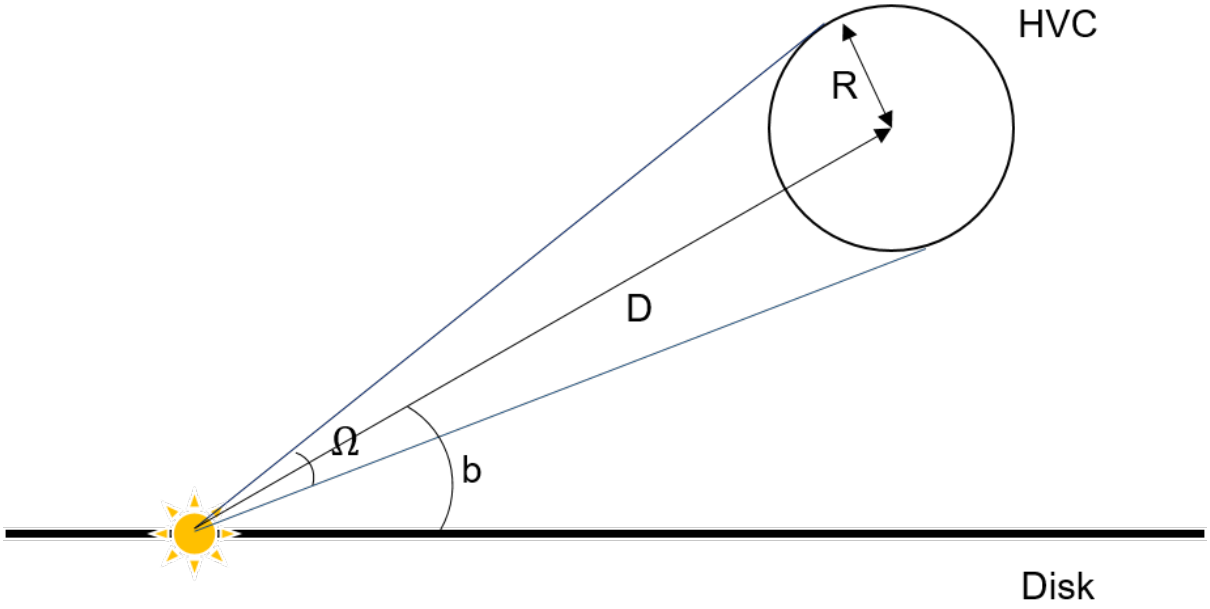

Figure 4: Schematic illustration of the infall parameters for a spherical HVC. D is the observed radial distance, Ω is the solid angle, and b is the galactic latitude. The area of detection, A, can be estimated from the distance and the solid angle which in turn is used for estimating the radius of the cloud from the following relation, $\Omega D^2 \sim A \sim R^2$.

the other as the intermediate case) for each complex, 4 different infall scenarios are constructed. A simulation run for the Complex C falling down towards the galactic disk is shown in Figure 3 as a representative example. The case is the maximum infall scenario (with the highest velocity and the largest density) among the 4 available setups where the vertical velocity and the HI volume number density are 143.9 km/s and 5.20×10^{-4} cm^{-3}, respectively.

4.2.3 Fuel Efficiency and Timescale

As an HVC complex is approaching to the galactic disk at an anomalous velocity, $v_{DEV} >$ 90km/s, a shock will be generated from the collision between the galactic disk and the complex. The forward shock that is propagating in the same direction of the complex and through the gaseous disk will have a velocity, v_{sd}, which can be estimated as,

$$v_{sd} = \frac{4}{3} \frac{1}{1 + \sqrt{\rho_d / \rho_{\rm HVC}}} v_{\rm HVC} \tag{4.39}$$

where ρ_d is the volume density of the galactic disk, $\rho_{\rm HVC}$ is the volume density of the HVC complex, and $v_{\rm HVC}$ is the velocity of the HVC complex [56–58]. Additionally, a rear shock is also generated from the collision. However, such shock will be ever-expanding in the direction back to the interstellar medium as gravitational fields, magnetic field, and cooling effects are neglected in the simulations. For such reason, only considered is the forward shock and the

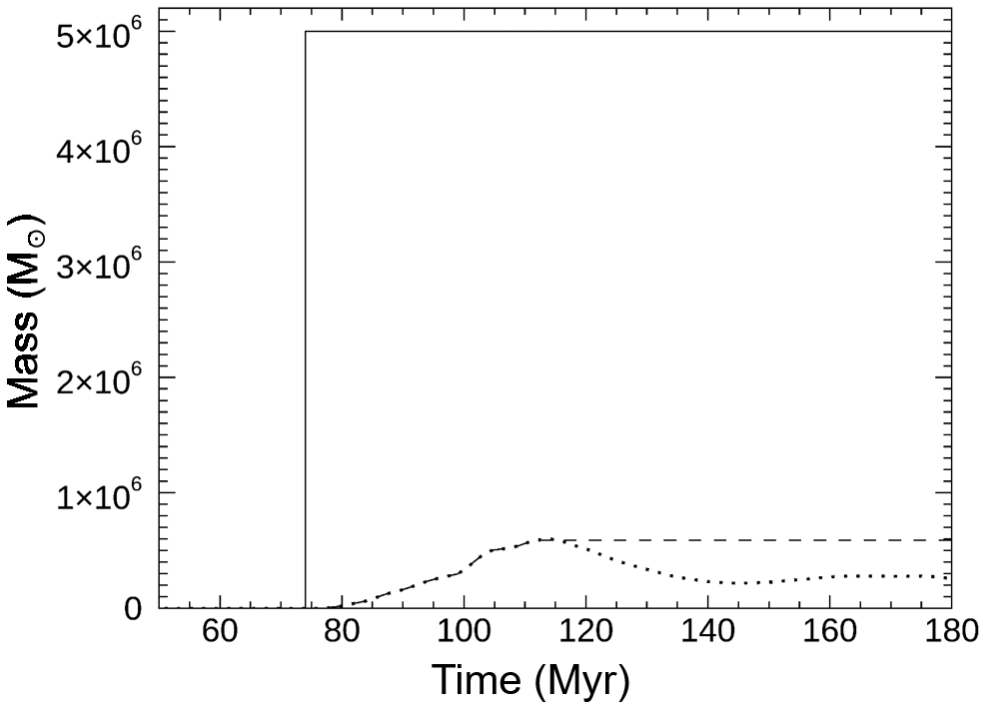

Figure 5: The amount of HVC mass supplied to the galactic disk from Complex C inflow as a function of time. The step-function like shape represents the mass infusion in the traditional infall scheme where the mass of the infalling complex is completely infused into the gaseous disk. The simulated amount of fuel supplied from the HVC complex is described in a dotted line, whereas the dashed line illustrates the fuel supply process when the long-term physical effects are not compensated from the characteristic timescale, $2\tau_{char}$, since impact.

characteristic time can be defined such as,

$$\tau_{char} = h_d / v_{sd} \tag{4.40}$$

where h_d is the thickness of the gaseous galactic disk.

As a method for approximating the long-term evolution, assumed is that the infusion of HVC material is completed at the time, $t_f = t_i + 2\tau_{char}$, where t_i is the time at impact (i.e. the point where the HVC material first reaches the gaseous disk). The time evolution of the amount of fuel infused into the galactic disk from the inflowing HVC material is investigated for such time span, t_f. The ratio between the total amount of fuel supplied and the initial amount of HVC material is defined as the "fuel efficiency". For example, the difference between the traditional accretion case and the fuel supply into the galactic disk from the inflow of Complex C is described in Figure 5. The plot is generated from the simulation results described in the previous Figure 3. The infall rate is shown as a step function-like structure due to the traditional assumption of complete accretion. The true supply rate of HVC mass is represented in a dotted

line. The dashed line illustrates how the estimation of fuel supply can alter when the long-term evolution is not compensated through the characteristic timescale. The fuel supply rate is clearly lower than the infall rate when the hydrodynamic interaction between the cloud and the disk is considered. This is primarily due to the density difference between the two gaseous objects where the density of the gaseous disk is higher than that of the inflowing HVC complex. Also identified is that the initially spherical HVC is horizontally compressed and a great amount of the material is returned back to the halo medium.

4.3 Simulation Results

4.3.1 Proof of the Idea

Two scenarios are constructed where a total of five HVCs identical in mass and size are falling down onto the galactic disk. The mass of the clouds is 1.0×10^5 $M_\odot$ and the HI volume number density is 1.0×10^{-2} cm^{-3}. In the first infall scenario, the initial velocity of the inflowing clouds is 100 km/s but the distance among the HVCs is increasing with an increment of 2 kpc beginning from 2 kpc up to 10 kpc. In the second infall scenario, the clouds are positioned at an initial distance of 4 kpc but the velocity among the HVCs varies from 40 km/s up to 120 km/s. The time evolution of HVC material in the disk from the two scenarios is given in Figure 6 and Figure 7. The supply of HVC material into the disk as a function of time in the traditional infall scenario is illustrated as a staircase function-like plot since complete accretion up until to the time to impact (D_i/v_i) is the underlying assumption. The time evolution of HVC fuel supply from the simulation results is illustrated by the dotted lines on the same (top) panels in Figure 6 and Figure 7 where the maximum supply of material from each HVC takes place at the peaks. The efficiency of total material supply from HVC inflow is 0.211 and 0.111 for the first and second infall cases. Presented in the panels at the bottom is the mass supply rate (i.e., the infall rate) from the inflowing HVCs estimated from Equation (3.35) at the time, $t = t_i + 2\tau_{char}$, which is the point when the process of HVC material infusion is considered completed for each inflowing clouds. The white diamonds represent the traditional infall rate while the black diamonds are the fuel supply rate estimated from the simulations. The average efficiency of the fuel supply rate for the first and second case is 0.217 and 0.246, respectively. It is implied from the efficiencies that both the supply rate and the total amount of supplied HVC material are overestimated in the traditional scheme of gas inflow.

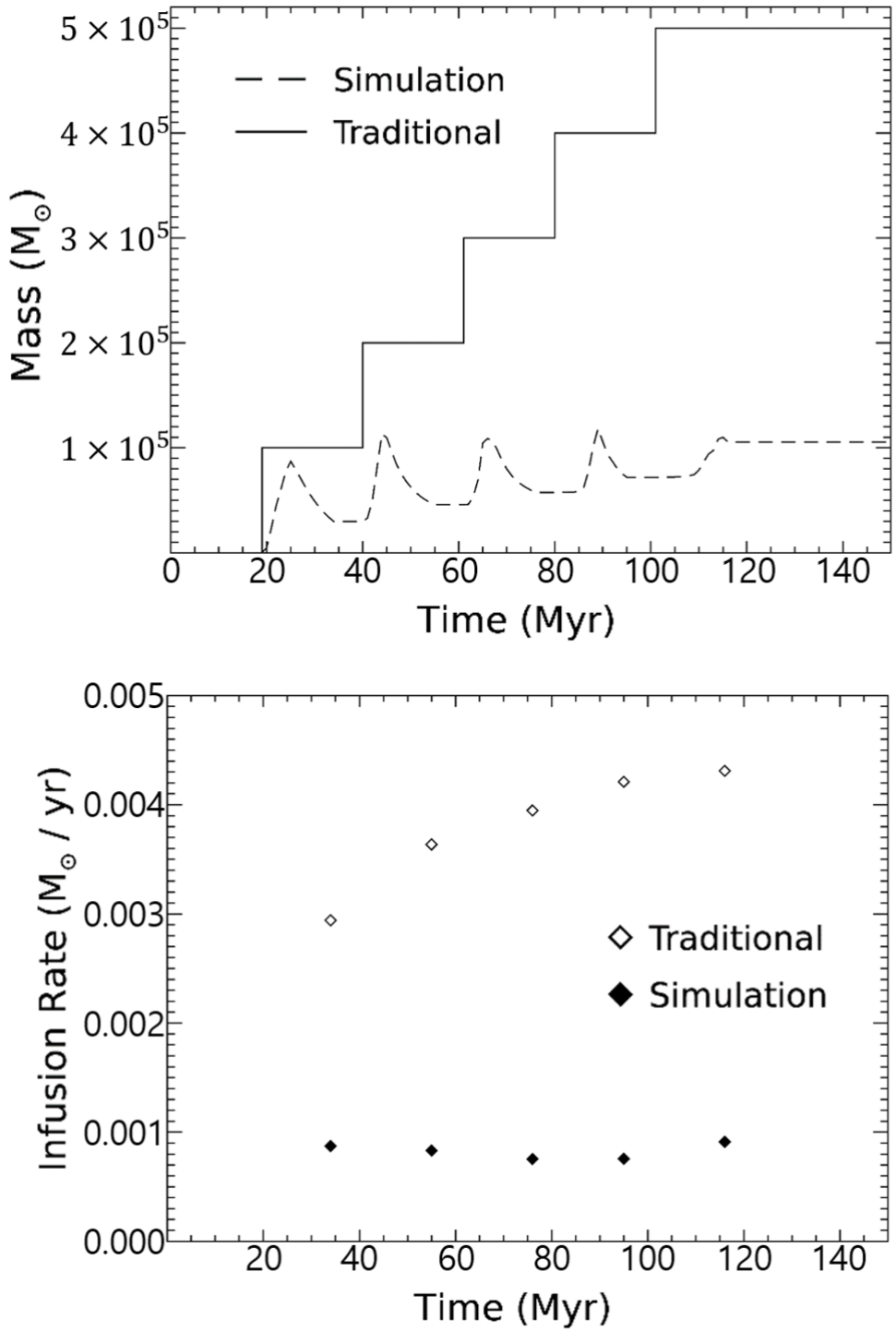

Figure 6: The first infall scenario, where five clouds with the same velocity but different distances are colliding with the galactic disk. The initial velocity of the inflowing clouds is 100 km/s and the distance is increased from 2 kpc up to 10 kpc with an increment of 2 kpc. The supply rate of HVC material is estimated at the times, $t = t_i + 2\tau_{char}$, for each inflowing HVC.

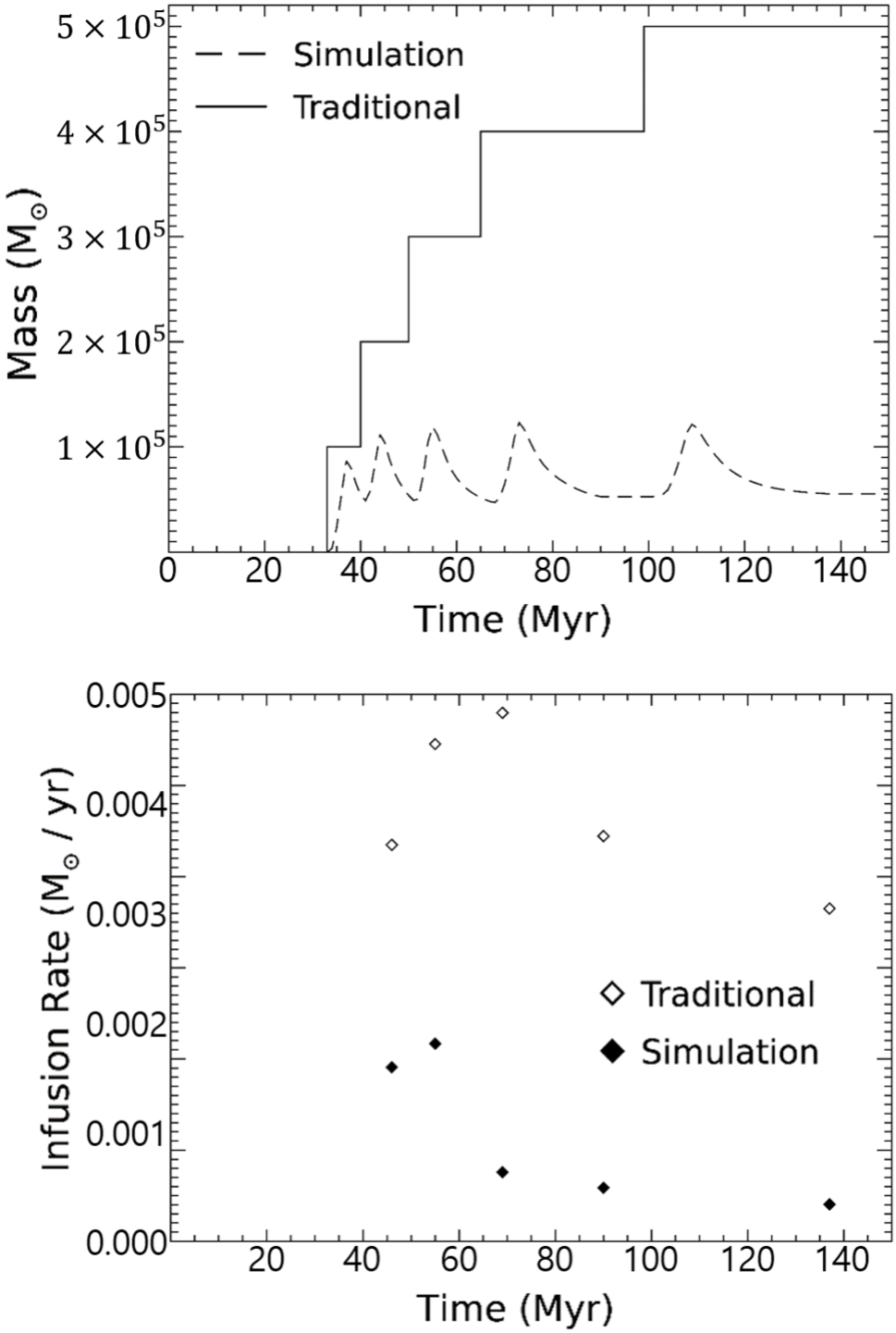

Figure 7: The second infall scenario, where the clouds are positioned at an initial distance of 4 kpc but the velocity among the HVCs varies from 40 km/s up to 120 km/s. The time evolution of the mass supplied to the gaseous disk (top panel) and the supply rate of HVC material estimated at the times, $t = t_i + 2\tau_{char}$, for each inflowing HVC (bottom panel).

4.3.2 HVC Infall Cases

Given the parameters for the 11 HVC complexes in Table 1, a total of four different inflow scenarios are constructed from the combinations between the two infall velocities and the two infall densities (intermediate and maximum extreme). Described in Figure 8 is the simulation result for all four infall scenarios considering the amount and the rate of HVC material supply into the galactic disk. The velocities of the HVC complexes in case 1 are identical to those in case 2, however, the infalling clouds experience different drag force and ram pressure while proceeding through the halo medium since the density is different between the two cases (case 1: extreme density, case 2: intermediate density). For that reason, the complexes in case 1 generally reach the galactic disk much quicker, in other words, have an earlier impact time compared to the complexes in case 1. Such a trend can also be observed between the infall cases 3 and 4 which share the same set of velocities but different radii and densities.

The traditional estimation of the amount of HVC material supplied into the disk as a function of time is described as a staircase function-like plots much like in the top panel of Figure 6 and Figure 7 while the dotted lines show the simulation results. The efficiency of material supply from the inflow of HVC complexes is 0.186, 0.044, 0.174, and 0.042 for the infall cases 1, 2, 3, and 4, respectively. The efficiency is comparable between the infall cases of 1 and 3 (also between cases 2 and 4) where the HVC complexes in the two infall cases share the same set of densities. The efficiency is also higher in the infall cases of 1 and 3 where the complexes have larger densities compared to those in the cases of 2 and 4. Such results imply that the efficiency of material supply from infalling HVC complexes depends dominantly on the density of clouds rather than on the velocity.

Shown in the bottom panel of Figure 8 is the rate of HVC material infusion at the time, $t = t_i + 2\tau_{char}$, when the process of HVC material infusion is considered completed for each inflowing HVC complex. The average efficiency of such rate of HVC material infusion is 0.249, 0.092, 0.247, and 0.072 for the infall cases 1, 2, 3, and 4, respectively. Once more, the average efficiency is comparable between the infall cases of 1 and 3 (also between cases 2 and 4) and also higher than the efficiency in the cases 2 and 4 without being affected by the large velocity difference in the HVC complexes.

In general terms, with the hydrodynamic interaction between the inflowing HVC complexes and the gaseous disk included, the supply rate and the total amount of supplied HVC material are overestimated in the traditional estimation of HVC inflow. The discrepancy is primarily due to the density difference between the complex and the disk. As the density of the galactic disk is always larger than the selected HVC complexes, the complex after impact is horizontally compressed and a good portion of the mass is returned back to the halo medium.

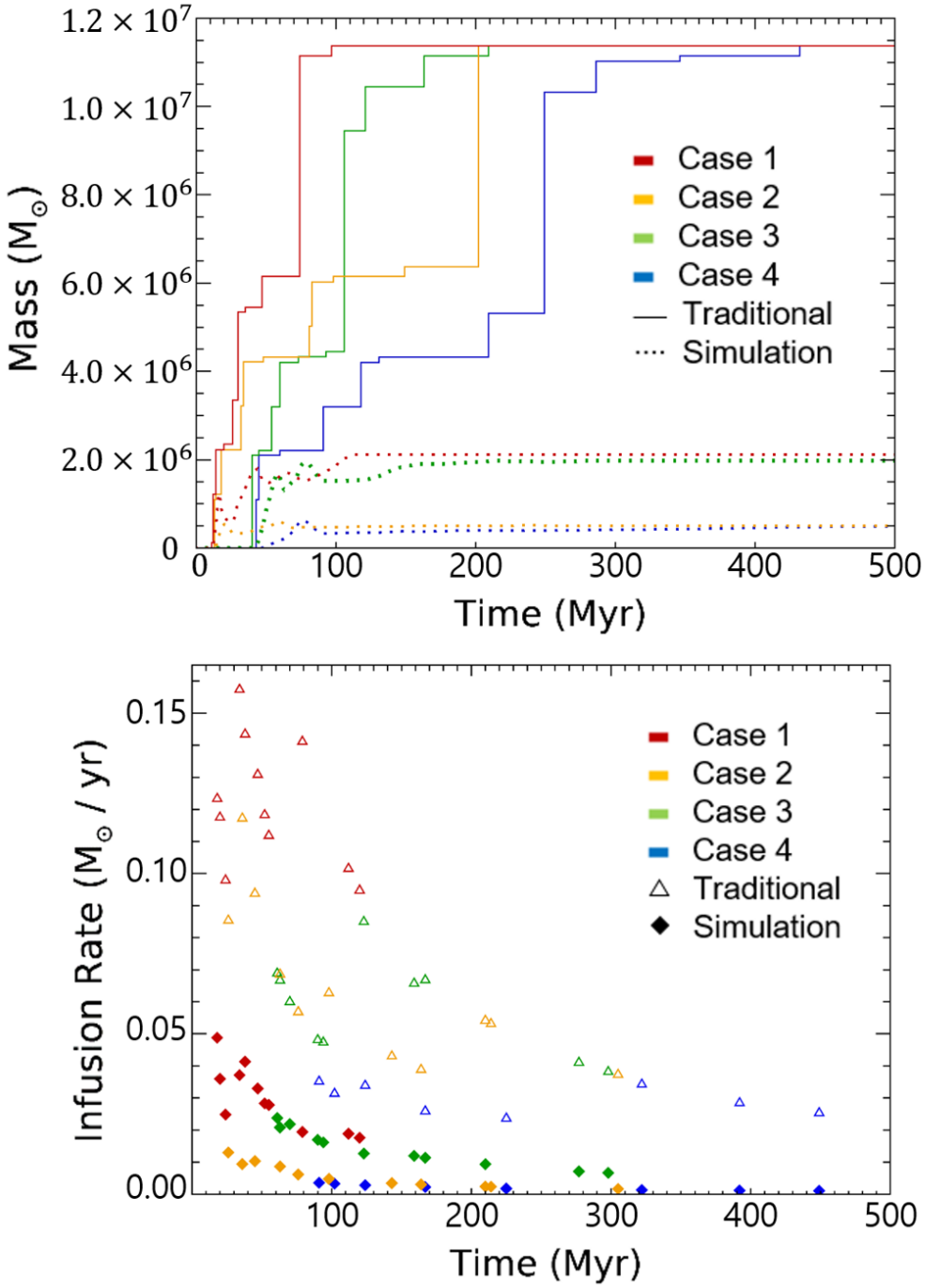

Figure 8: Time evolution of the mass supplied into the galatic disk (top) and the rate of mass supply at the time, $t = t_i + 2\tau_{char}$, for each inflowing complex (bottom). A total of 4 different inflow scenarios are constructed for the infall of 11 different HVC complexes. Case 1 (red): complexes with maximum velocity and density. Case 2 (yellow): maximum velocity but intermediate density. Case 3 (green): intermediate velocity but maximum density. Case 4 (blue): both intermediate velocity and density.

4.3.3 Limitations

Including the gravitational fields, self-gravity, magnetic fields, cooling effect and all other physical processes is essential for understanding the hydrodynamic mixing of gas between the inflowing HVC complexes and the gaseous disk. However, such processes are neglected in the current simulations. For that reason, the infall scenarios investigated in this study could be considered as only a toy model and the long-term dynamical evolution of material infusion under the effect of the essential physical processes would be different from the current simulation results. In order to compensate for the missing effects, a characteristic timescale is defined to deal only with the early dynamical interactions between the complexes and the gaseous disk. Nonetheless, the simulation in this study must be significantly improved to obtain better estimations of the true fuel supply rate which is the key for later predicting the number of stars formed from HVC infall. Discussed in the list below is how the fuel supply rate could be different from the current estimation if the simulation has included more realistic processes.

(1) The density is non-uniform for the inflowing HVCs, gaseous disk, and halo medium: Imagine that the HVC complex is no longer uniform in density but has a dense core and the density is lower at the boundaries. Similarly, the galactic has a dense center-layer of gas and the halo medium has a density gradient where the density is lower further away from the disk. The gas at the outside edge of the HVCs will blend in the halo medium from shear instabilities before reaching the galactic disk [59]. In this case, the efficiency will be lower than the current estimation. However, the dense core of the HVC complexes will also penetrate deeper into the disk allowing more material to interact with the gas within the gaseous disk and the efficiency should increase in such case.

(2) The galactic gravitational field is included: Not only in an astrophysical surrounding but in almost every situation, gravity is considered a fundamental element to be included. Yet, the hydrodynamic interaction can be dominant over gravity in the early stage of gas interaction. Therefore, expected is that the effect of gravitational fields to be more substantial during the later stage of the infusion process beyond the time, $2\tau_{char}$. In general, the efficiency should increase as the material left near the disk would eventually "stick" on the galactic disk. Another point to consider is the acceleration due to gravity. The impact velocity will be higher in the presence of gravity and therefore both the forward and rear shock will also be increased. While the penetration of the complex depends greater on the density difference, the interaction timescale would be dramatically changed from the altered infall velocity.

(3) Considering the magnetic field: Depending on the field orientation, the effect of magnetic fields on the efficiency can be extremely complicated. In some cases, the growth of shear instabilities could be restrained from the magnetic fields [60,61]. The efficiency is increased in such cases as the shape and mass of the HVC complexes are preserved better throughout

the progression in the halo medium. In the other case, where the field orientation is perpendicular to the velocity of the inflowing complex, the magnetic field lines are compressed and the supply of HVC material can be restrained [33, 62].

(4) The cooling of gas during and after the HVC-disk collision: Without cooling, the rear shock that is generated from the collision is continuously expanding back away from the disk and into the halo medium. In the case where the radiative cooling of gas is included, the material propagating back into the halo medium will blend into the halo medium at a location closer to the gaseous disk. From that point, the HVC material located near the gaseous disk can stick back onto the disk due to gravity and the increase in the efficiency is expected in such case.

(5) Determining the true path of the HVC infall: The HVC complexes are vertically dropping down on the galactic disk in the current simulations. In the case of a non-vertical HVC infall, the characteristic timescale should be redefined as the material will be travelling a longer distance throughout the gaseous disk. In such a case, for a longer time of gas mixing, the amount of material left in the disk should increase as cooling and gravity are effective during the later stage of the infusion process. However, the efficiency would also depend on the orientation of the magnetic fields and the composition of the infalling complexes.

V Conclusion and Future work

The study in this thesis is driven from the idea that full and steady accretion of material on the galactic disk from HVC infall is unlikely due to the hydrodynamic interaction between the inflowing cloud and the gaseous disk. In order to prove the idea, constructed are four different infall scenarios for a total of eleven HVC complexes depending on the density, size and velocity configuration of the inflowing complexes. It is shown in all four infall cases that the mass supply rate on the galactic disk is overestimated in the traditional interpretation of mass infall compared to the simulation results that include the hydrodynamic interaction between the disk and the cloud. The efficiency of the HVC material supply rate can be as low as ~ 0.072 compared to the traditional estimation where full accretion of mass is the underlying assumption. The results also show that the efficiency of material supply from infalling HVC complexes depends more significantly on the density of clouds rather than on the velocity. Expected is that such inefficiency of fuel supply through HVC material inflow which is shown from the current simulations to be valid also in the presence of the gravitational fields, cooling effects, and magnetic fields that were neglected.

The ultimate objective is to improve the GCE model prediction on the evolution history of chemical abundances by introducing the number of stars formed through the extra material provided by HVC infall. The star formation in a galaxy can be triggered by both the inflow and outflow of gas [63]. The momentum and material from HVC collision can be a good source

of both inflow and outflow and the true amount and rate of material supply covered in this study can serve as a groundwork for further implications. However, there is only little known regarding the detailed process of star formation in a galaxy. A simple idea is to estimate the amount of molecular gas supplied from HVC infall. Such work requires further investigation on the relationship between dust and HI$-H_2$ conversion.

Appendix A

Derivation of the Initial Mass Function (IMF)

The mass distribution of stars per unit area, $n(m)$, at the current time for the stars with the mass $0.1\mathrm{M}_\odot < m < 1.0\mathrm{M}_\odot$ is

$$n(m) = \int_0^{t_G} \varphi(m)\psi(t)\mathrm{d}t \tag{A.1}$$

where the lifetime of the stars is larger than or equal to the age of the galaxy so that $\tau_m \geq t_G$.

Assuming that initial mass function, $\varphi(m)$ is time invariant and the stars are in the main sequence, we have,

$$n(m) = \varphi(m)\ \overline{\psi}\ t_G \tag{A.2}$$

where $\overline{\psi}$ is the time average star formation rate.

Now considered is the current time mass distribution of stars per unit area with their lifetimes $\tau_m << t_G$ and mass $m \geq 2\mathrm{M}_\odot$.

$$n(m) = \int_{t_G-\tau_m}^{t_G} \varphi(m)\psi(t)\mathrm{d}t \tag{A.3}$$

Koppen et al 1995 star formation rate With the same assumption of having a time independent initial mass function, Equation (A.3) becomes,

$$n(m) = \varphi(m)\psi(t_G)\tau_m \tag{A.4}$$

where $\psi(t_G)$ is the star formation rate found today so that $\psi(t_G) = \psi(t_G - \tau_m)$.

Remaining is the stars in the range of $1\mathrm{M}_\odot < m < 2\mathrm{M}_\odot$, where the assumptions based on the stellar lifetimes do not hold. For such reason, the IMF, $b(t_G)$ in this range of mass is estimated from the ratio of the star formation rate at present time to the total galactic time averaged SFR, $\overline{\psi_G}$.

$$b(t_G) = \frac{\psi(t_G)}{\overline{\psi_G}} \tag{A.5}$$

Required is $0.5 \leq b(t_G) \leq 1.5$ to have $\varphi(m)$ reasonably well-fit in the range of $1\mathrm{M}_\odot < m < 2\mathrm{M}_\odot$ [64]. The estimated range for $b(t_G)$ implies that the star formation rate should be marginally decreasing in time. By investigating the age distribution of the F stars in the local

galactic disk it was found that the SFR at the present time is ~ 0.67 of the average SFR at about 12 Gyrs ago [65]. This was later recalculated considering the scale height. Assuming that the increase in scale height is proportional to the dispersion in velocity, the present time SFR is ~ 0.42 compared to the past SFR. It is also known that the SFR could fluctuate on timescales $< 0.2 \sim 1.0$ Gyr more than a factor of $2 \sim 3$ [66], nonetheless, the overall time average SFR is generally favored in GCE. Therefore, deriving the chemical abundance in stars and gas in terms of the star formation rate and initial mass function is still a work in progress and needs to be further tested.

Appendix B

Parameterization and Derivation of the Star Formation Rate (SFR)

The formation of a star is a very complicated physical process where we know only a little regarding the conditions of stellar birth. It is considered that the physical processes such as cloud collisions, magnetic fields, gas rotation, metallicity, shear instability, and spiral shocks can be involved in the process of star formation, however, the total density of the gas is considered to be the most significant factor for the SFR.

The most famous and convenient way of estimating the star formation rate was suggested by Schmidt (1959;1963) [17, 19] where the rate is parameterized such as,

$$\psi(t) \propto \rho_{\rm gas}^{k} \tag{B.1}$$

where $\rho_{\rm gas}$ is the volume gas density and k is in the range of $1-2$.

However, the scale height of the gas which is difficult to measure can be ignored by using the surface gas density instead of the volume gas density so that,

$$\psi(t) \propto \sigma_{\rm gas}^{k} \tag{B.2}$$

where σ_{gas} is the surface gas density. While the Equation (B.1) does not include molecular hydrogen, the surface gas density is estimated as $1.4(\mathrm{HI}+\mathrm{H_2})$ where the factor 1.4 indicated the contribution of helium.

The estimation of SFR has been developed and refined ever since. Notable efforts include using the total surface gas density instead of only molecular gas density [67,68], considering the metallicity dependence [69, 70], using both the surface gas density and the surface mass density [71, 72], and considering cold gas only [73, 74].

Widely accepted in GCE models is an exponentially decreasing star formation rate which can be expressed as,

$$\psi(t) \propto e^{-t/\tau} \tag{B.3}$$

where τ is a free parameter in the range of $5-15$ Gyr in order to have the estimation consistent with observational constraints [6].

As mentioned in Section 1.2.1 the IMF must be pre-defined in order to derive the star formation rate, $\psi(t_G)$. With reasonable initial mass functions, first calculated by Miller and Scalo (1979) [75] and extensively summarized by Timmes et al. (1995) [76], the local star formation rate at present time is estimated as following.

$$\psi(t_G) \sim 2-10\ \mathrm{M_\odot pc^{-2}Gyr^{-1}} \tag{B.4}$$

However, the tracers that can be used for estimating the SFR are limited to the massive stars in the mass range of $5 - 10$ $M_{\odot}$ which converts to about $5 - 20\%$ of the total stellar mass. This leaves one to estimate the SFR through a heavy extrapolation over the observed stellar population.

Appendix C

Stellar Yield

The "yield" is defined as the ratio of the synthesized and ejected elements to the chemical elements remaining in the remnants [77]. Underlying the definition is the assumption of instantaneous recycling and homogeneous mixing so that the lifetime of the stars with mass $m \geq 1M_{\odot}$ can be ignored and all other stars that are low-mass with $m < 1M_{\odot}$ has a very long lifetime that is comparable to the lifetime of a galaxy. Such approximation, so-called the IRA is widely used in GCE models in order to obtain an analytic solution for the chemical enrichment in a given galactic system. Similar but different is the definition of "stellar yield" which is the total mass of metals synthesized and then ejected from a star of metallicity Z. The stellar yield can be estimated in many different ways depending on the mass of the star; whether it is massive or low in mass, on the type of ejecta; whether the ejection of metals is originated from Type I SN, Type II SN or stellar winds. Detailed parameters considered in the estimation of such yield include the mass of the helium core, the carbon-oxygen core mass, and the mass of the remnant.

Widely used is the stellar production matrix (Talbot and Arnett 1973) which is very useful in terms of expressing the production and ejection of chemical elements, so defined as,

$$Q_{ij}(m) = \frac{(m_{ej})_{ij}(m)}{mX_j} \tag{C.1}$$

where $(m_{ej})_{ij}(m)$ describes the ejected mass of element i which was originally existing in the form of j before nucleosynthesis. X_j represents the abundance of element j at the birth of such star.

Then the total mass contribution from the ejection of both the newly synthesized and the pre-existing elemental component i can be given as,

$$(M_{ej})_i = \sum_{j=1,n} Q_{ij}(m) X_j m \tag{C.2}$$

so that the abundance of the ISM is equivalent to the abundance X_j when a star is born.

In most of the cases, the matrix depends on the chemical composition at the initial state. Furthermore, mass fractions in the process of nucleosynthesis such as the mass fraction participating in hydrogen burning, the mass fraction of helium burning, and the mass fraction of the transformation of heavier elements and many more must be defined to estimate the yield together with the production matrix.

From the stellar production matrix and the nucleosynthetic mass fractions, obtained is the "galactic yield", y_i which is estimated as,

$$y_i = \frac{1}{1-R} \int_1^{\infty} m p_{im} \varphi(m) \mathrm{d}m \tag{C.3}$$

where $p_{im} = \frac{(M_{ej})_i}{m}$ and R is the total mass fraction of the chemical elements from a stellar generation that is returned back into the gas defined as following.

$$R = \int_1^{\infty} (m - M_R)\varphi(m)\mathrm{d}m \tag{C.4}$$

The total fraction of returned material, R, depends on the IMF and the $(m - M_R)$ relation which is assumed as [77],

$$M_R = 0.7\mathrm{M}_{\odot} \qquad \text{where } m \leq 4\mathrm{M}_{\odot} \tag{C.5}$$

$$M_R = 1.4\mathrm{M}_{\odot} \qquad \text{where } m > 4\mathrm{M}_{\odot} \tag{C.6}$$

but also could be estimated from the semi-empirical relation as following [78].

$$M_R = 0.05m + 0.5 \quad \text{where } 1\mathrm{M}_{\odot} \leq m < 6\mathrm{M}_{\odot} \tag{C.7}$$

$$M_R = 0.144m \qquad \text{where } 6\mathrm{M}_{\odot} \leq m < \mathrm{M}_{\mathrm{up}} \tag{C.8}$$

where $\mathrm{M}_{\mathrm{up}} \sim 4 - 5\ \mathrm{M}_{\odot}$ is the mass at the third dredge-up.

Appendix D

Formulation and Derivation of the Simple Model of Chemical Evolution

The brief description of the Simple Model of GCE was made in Section (2.2), but here more detailed one is given with additional equations. Following the same assumptions listed in Section (2.2.1), imagine a box within a galactic system that is homogeneous with plenty of stars from various generations. In such a volume, the total mass $M_{\rm total}$ is the sum of the mass of stars $M_{\rm stars}$ and the mass of gas $M_{\rm gas}$ so that,

$$M_{\rm total}(t) = M_{\rm stars}(t) + M_{\rm gas}(t) \tag{D.1}$$

at time t. From below we write $M_{\rm stars} = M_{\rm stars}(t)$ and $M_{\rm gas} = M_{\rm gas}(t)$ for the sake of simplicity in the notations. The initial conditions at time $t = 0$ is $M_{\rm stars}(0) = 0$ and $M_{\rm total} = M_{\rm gas}(0)$.

Defining the mass of metals in the gas as $M_{\rm metals}$, the mass fraction of heavy elements, also known as the metallicity is,

$$Z = \frac{M_{\rm metals}}{M_{\rm gas}} \tag{D.2}$$

at time t, where we also write $M_{\rm metals} = M_{\rm metals}(t)$.

Say that stellar birth occurs within the time interval of $t \sim t + \delta t$, so that the change in stellar mass and gas is $\delta M_{\rm stars}$ and $\delta M_{\rm gas}$, respectively. The primary objective is to describe the metallicity change, δZ in terms of the mass change in stars and the mass change in gas.

Starting from the time differential of Z,

$$\frac{{\rm d}Z}{{\rm d}t} = \frac{\partial Z}{\partial M_{\rm metals}}\frac{{\rm d}M_{\rm metals}}{{\rm d}t} - \frac{\partial Z}{\partial M_{\rm gas}}\frac{{\rm d}M_{\rm gas}}{{\rm d}t} \quad . \tag{D.3}$$

and the differential of Equation (D.2),

$$\frac{\partial Z}{\partial M_{\rm metals}} = \frac{1}{M_{\rm gas}} \tag{D.4}$$

$$\frac{\partial Z}{\partial M_{\rm gas}} = -\frac{M_{\rm metals}}{M_{\rm gas}^2} \tag{D.5}$$

we have,

$$\frac{{\rm d}Z}{{\rm d}t} = \frac{1}{M_{\rm gas}}\frac{{\rm d}M_{\rm metals}}{{\rm d}t} - \frac{M_{\rm metals}}{M_{\rm gas}^2}\frac{{\rm d}M_{\rm gas}}{{\rm d}t} \quad . \tag{D.6}$$

For a small time interval ∂t,

$$\partial Z = \frac{\partial M_{\rm metals}}{M_{\rm gas}} - \frac{M_{\rm metals}}{M_{\rm gas}^2}\partial M_{\rm gas} \tag{D.7}$$

and such can be rearranged using the definition of Z in Equation (D.2) so that we obtain the following expression.

$$\partial Z = \frac{\partial M_{\rm metals}}{M_{\rm gas}} - Z\frac{\partial M_{\rm gas}}{M_{\rm gas}} \tag{D.8}$$

The total mass "undergoing" the process of star formation is defined as $M_{\rm SF}$ to be distinguished from the total mass "in" the stars, $M_{\rm stars}$ so that $M_{\rm SF} > M_{\rm stars}$. Defining α as the fraction of mass that remains in the stars with a very long lifetime, we have,

$$\partial M_{\rm stars} = \alpha \partial M_{\rm SF} \tag{D.9}$$

where $0 < \alpha < 1$.

The total mass of newly synthesized metals that are ejected back as gas is assumed proportional to the total stellar mass. The synthesized and then ejected mass is defined as $p\partial M_{\rm stars}$, where p here is a constant yield.

By the assumption, the change in the mass of metals $\partial M_{\rm metals}$ during a very short time ∂t is due to the combination of metal ejecta after stellar nucleosynthesis and star formation from the gas containing such metals. Therefore, in a very short time ∂t we have,

$$\partial M_{\rm metals} = -Z\partial M_{\rm SF} + Z(1-\alpha)\partial M_{\rm SF} + p\partial M_{\rm stars} \tag{D.10}$$

where the first term on the right side of the equation is the loss of metals due to star formation, the second term is the contribution from the ejecta of unchanged metals, and the last term describes the ejected metals that are newly synthesized.

From the definitions, the Equation (D.10) can be re-arranged as,

$$\partial M_{\rm metals} = -Z\alpha\partial M_{\rm SF} + p\partial M_{\rm stars} \tag{D.11}$$

$$= -Z\partial M_{\rm stars} + p\partial M_{\rm stars} \tag{D.12}$$

which can be further devided by $M_{\rm gas}$ and give

$$\frac{\partial M_{\rm metals}}{M_{\rm gas}} = -Z\frac{\partial M_{\rm stars}}{M_{\rm gas}} + p\frac{\partial M_{\rm stars}}{M_{\rm gas}} \quad . \tag{D.13}$$

However, for a closed box the relation $\partial M_{\rm total} = \partial M_{\rm stars} + \partial M_{\rm gas} = 0$ holds and we have,

$$\frac{\partial M_{\rm metals}}{M_{\rm gas}} = Z\frac{\partial M_{\rm gas}}{M_{\rm gas}} - p\frac{\partial M_{\rm gas}}{M_{\rm gas}} \tag{D.14}$$

which can be substituted into Equation (D.8) so that we obtain,

$$\partial Z = Z\frac{\partial M_{\rm gas}}{M_{\rm gas}} - p\frac{\partial M_{\rm gas}}{M_{\rm gas}} - Z\frac{\partial M_{\rm gas}}{M_{\rm gas}} \tag{D.15}$$

$$= -p\frac{\partial M_{\rm gas}}{M_{\rm gas}} \quad . \tag{D.16}$$

Now Equation (D.16) is converted to a differential and then time integrated from 0 to t such as,

$$\int_0^{Z(t)} {\rm d}Z' = -\int_{M_{\rm gas}(0)}^{M_{\rm gas}(t)} p\frac{{\rm d}M'_{\rm gas}}{M'_{\rm gas}} \tag{D.17}$$

so that we obtain the following relation.

$$Z(t) = -p\ln\frac{M_{\rm gas}(t)}{M_{\rm gas}(0)} \tag{D.18}$$

In terms of gas fraction, μ, Equation (D.18) can be re-written as,

$$Z(t) = -p\ln\mu \tag{D.19}$$

and we obtain the final analytical solution for the Simple Model of chemical evolution.

Appendix E

Further Complicated Galactic Chemical Evolution Models

Considering the Gas Flow

The metal enrichment where the system allows gas flow can be described as,

$$\frac{\mathrm{d}(ZM_{\mathrm{gas}})}{\mathrm{d}t} = -Z(t)\psi(t) + E_Z(t) + Z_A A(t) - Z(t)W(t) \tag{E.1}$$

where $W(t)$ is the material loss rate and $A(t)$ is the accretion rate of the material of metal fraction Z_A

(1) Considering only the outflow at this moment we have,

$$\frac{\mathrm{d}M_{\mathrm{total}}}{\mathrm{d}t} = -W(t) \tag{E.2}$$

$$\frac{\mathrm{d}M_{\mathrm{gas}}}{\mathrm{d}t} = -(1-R)\psi(t) - W(t) \tag{E.3}$$

$$\frac{\mathrm{d}(ZM_{\mathrm{gas}})}{\mathrm{d}t} = -(1-R)\psi(t)Z(t) + y_Z(1-R)\psi(t) - Z(t)W(t) \quad . \tag{E.4}$$

The material loss from the wind, $W(t)$, is assumed proportional to the rate of material recycling and the SFR with the presence of a constant λ such as,

$$W(t) = \lambda(1-R)\psi(t) \tag{E.5}$$

where $\lambda \geq 0$ is the parameter for the wind. After going through the similar algebraical work as in the simple model case, we obtain,

$$\frac{\mathrm{d}Z}{\mathrm{d}M_{\mathrm{gas}}} = -\frac{y_Z}{M_{\mathrm{gas}}(1+\lambda)} \tag{E.6}$$

which can also be integrated from $Z(0)$ to $Z(t)$ and from $M_{\mathrm{gas}}(0)$ to $M_{\mathrm{gas}}(t)$ to obtain the analytical solution as in the simple model. After such integration we have,

$$Z = -\frac{y_Z}{1+\lambda}\ln[M_{\mathrm{gas}}(t)/M_{\mathrm{gas}}(0)] \tag{E.7}$$

where the mass of gas at the initial state can be expressed as,

$$M_{\mathrm{gas}}(0) = (\lambda+1)M_{\mathrm{total}}(t) - \lambda M_{\mathrm{gas}}(t) \tag{E.8}$$

so that we obtain the anaylitical solution for the "outflow only" case as following.

$$Z = \frac{y_Z}{1+\lambda}\ln[(1+\lambda)\mu^{-1} - \lambda] \tag{E.9}$$

(2) Now considering only the inflow we have,

$$\frac{\mathrm{d}M_{\mathrm{total}}}{\mathrm{d}t} = A(t) \tag{E.10}$$

$$\frac{\mathrm{d}M_{\mathrm{gas}}}{\mathrm{d}t} = -(1-R)\psi(t) + A(t) \tag{E.11}$$

$$\frac{\mathrm{d}(ZM_{\mathrm{gas}})}{\mathrm{d}t} = -(1-R)\psi(t)Z(t) + y_Z(1-R)\psi(t) + Z_A A(t) \quad . \tag{E.12}$$

The accretion rate $A(t)$ is assumed as,

$$A(t) = \Lambda(1-R)\psi(t) \tag{E.13}$$

where $\Lambda > 0$. Also through the similar algebraical work as in the simple model case, we obtain,

$$M_{\mathrm{gas}}\frac{\mathrm{d}Z}{\mathrm{d}t} = y_Z(1-R)\psi(t) + (Z_A - Z)A(t) \quad . \tag{E.14}$$

Considering only primordial material where $Z_A = 0$ and $\Lambda \neq 1$ we have,

$$Z = \frac{y_Z}{\Lambda}[1 - (\Lambda - (\Lambda-1)\mu^{-1})^{-\Lambda/(1-\Lambda)}] \quad . \tag{E.15}$$

The "extreme" infall model is equivalent to the case where $\Lambda = 1$ [79].

(3) Finally, considering both outflow and inflow, the analytic solution is as following.

$$Z = \frac{y_Z}{\Lambda}[1 - \{(\Lambda-\lambda) - (\Lambda-\lambda-1)\mu^{-1})\}^{\Lambda/(\Lambda-\lambda-1)}]\} \quad . \tag{E.16}$$

Biased Galactic Winds

It is widely accepted that metal-enhanced galactic winds are produced from a galaxy by supernovae explosions. In such case, the galactic wind rate is defined as,

$$W(t)Z^{\circ} = \alpha Z\lambda(1-R)\psi(t) \tag{E.17}$$

where Z° is the metallicity of the outflowing material. Z° can be addressed in the form of the galactic metallicity Z such as,

$$Z^{\circ} = \alpha Z \tag{E.18}$$

where α is the efficiency of ejection > 1. Then we define the time evolution of chemical enrichment as,

$$\frac{\mathrm{d}(ZM_{\mathrm{gas}})}{\mathrm{d}t} = (1-R)\psi(t)[\Lambda Z_A + y_Z - (\lambda\alpha + 1)Z] \tag{E.19}$$

where λ, Λ, and Z_A follows the same definition as in the previous derivation of the gas flow model.

The analytical solution is given as [80],

$$Z = \frac{\Lambda Z_A + y_Z}{\Lambda + (\alpha-1)\lambda}[1 - \{(\Lambda-\lambda) - (\Lambda-\lambda-1)\mu^{-1}\}^{\frac{\Lambda+(\alpha-1)\lambda}{\Lambda-\lambda-1}}] \tag{E.20}$$

however, the analytical solution only holds for primary elements.

Galactic Fountains

It is similar to the case of biased galactic winds but the direction of gas flow is opposite as metal-rich material is infalling into the system. In such case we define,

$$Z_A = Z^\circ = \alpha Z \tag{E.21}$$

so that the metal fraction of the inflowing gas is equal to the galactic wind case. Additionally assumed is $\lambda \geq \Lambda$ as the gas inflowing to the system is originated from the gas from winds. Then the analytical solution is given as following [80].

$$Z = \frac{y_Z}{(\lambda - \Lambda)(\alpha - 1)}[1 - \{(\Lambda - \lambda) - (\Lambda - \lambda - 1)\mu^{-1}\}^{\frac{(\lambda-\Lambda)(\alpha-1)}{\Lambda-\lambda-1}}] \tag{E.22}$$

Radial Flows

In spiral disks, the transfer of angular momentum from gravitation and/or viscosity generates radial flows. Such process plays a role in GCE as the flow will create a tendency of higher-metallicity in the direction towards the center of the disk which can be one of the factors of metallicity gradients in the galactic disk.

Considering a ring in a galactic disk between r and $r + \delta r$, we can re-address the equations in the simple model by substituting $M_{\rm gas} = 2\pi r M_{\rm gas}\delta r$ and $\psi = 2\pi r\psi\delta r$. Using the surface density, the radial flow, F, is expressed as,

$$F(r) - F(r + \delta r) = -(\partial F/\partial r)\delta r \tag{E.23}$$

where F is in the unit of $\mathrm{M_\odot yr^{-1}}$ and the direction of flow is determined by the positive/negative sign (outward/inward).

Then the flow of metals is defined such as following.

$$Z(r)F(r) - Z(r + \delta r)F(r + \delta r) = -Z(\partial F/\partial r)\delta r - (\partial Z/\partial r)F\delta r \tag{E.24}$$

We use the definition and substitute the infall and outflow term with F to obtain,

$$\frac{\partial M_{\rm gas}}{\partial t} = -(1 - R)\psi - \frac{1}{2\pi r}\frac{\partial F}{\partial r} \tag{E.25}$$

$$M_{\rm gas}\frac{\partial Z}{\partial t} = y_Z(1 - R)\psi - \frac{1}{2\pi r}\frac{\partial Z}{\partial r}F \quad . \tag{E.26}$$

The radial flow is consistent with near steady-state metallicity gradient such as,

$$\frac{\partial(Z/y_Z)}{\partial r} \sim 2\pi r\frac{(1 - R)\psi}{F} \tag{E.27}$$

where the inward flow is in interest for the case of spiral galaxies.

The metallicity, Z, can be changed by the radial flow on a timescale defined as,

$$\tau_F \sim 2\pi r^2\frac{M_{\rm gas}}{|F|} \tag{E.28}$$

where the flow, F, can also be estimated in terms of the velocity of the flow such as,

$$|F| = 2\pi r M_{\rm gas}|v_F| \quad . \tag{E.29}$$

Then the radial flow timescale is now expressed as,

$$\tau_F \sim \frac{r}{|v_F|} \tag{E.30}$$

which leads to the relation,

$$\frac{\partial(Z/y_Z)}{\partial \ln r} \sim \frac{\tau_F}{\tau_{\rm star}} \tag{E.31}$$

where $\tau_{\rm star}$ is the star formation timescale, also known as the time required for gas depletion.

Since τ_F is inversely proportional to the velocity of gas flow, it is implied that the abundance gradient is promoted from a slow gas flow. A number of studies suggest that at flow velocities, $|v_F| > 2$ km/s, the metallicity gradient would disappear. However, there is yet none observationally confirmed regarding the radial flows.

Comprehensive Equation of Chemical Evolution

Based on the derivations of yield and the stellar production matrix, gas inflow and outflow, galactic winds and fountains, and radial flows we now attempt to drop the assumption of instantaneous recycling and obtain a comprehensive equation that describes the chemical enrichment as a function of time. Considering a chemical element, i, an integral-differential equation can be written as following.

$$\begin{aligned}
\dot{M}_i(t) = &- \psi(t) X_i(t) + \int_{M_L}^{M_{Bm}} \psi(t-\tau_m) Q_{mi}(t-\tau_m) \varphi(m) dm \\
&+ A_B \int_{M_{Bm}}^{M_{BM}} \varphi(m) [\int_{\mu B_{min}}^{0.5} f(\mu_B) \psi(t-\tau_{m2}) Q_{mi}(t-\tau_{m2}) d\mu_B] dm \\
&+ (1-A_B) \int_{M_{Bm}}^{M_{BM}} \psi(t-\tau_m) Q_{mi}(t-\tau_m) \varphi(m) dm \\
&+ \int_{M_{BM}}^{M_U} \psi(t-\tau_m) Q_{mi}(t-\tau_m) \varphi(m) dm + X_{iA}(t) A(t) \\
&- X_i(t) W(t) + X_i(t) I(t)
\end{aligned} \tag{E.32}$$

where $X_i(t) = \frac{\sigma_i(t)}{\sigma_{\rm gas}(t)} = \frac{M_i(t)}{M_{\rm gas}(t)}$ is the mass abundance of the element i and σ_i is the surface gas density of the element i.

The first term in Equation (E.32) is the rate of chemical elements removed from the gas and involved in star formation. The following integrals are the rate of chemical elements being restored back to the ISM from various types of supernovae explosions, binary systems, galactic wind, accretion. The first integration describes the contribution of single stars in the mass range of $M_L - M_{Bm}$ where $M_L \sim 0.8 M_\odot$ is the minimum mass. The second integration is the contribution of Type Ia SNe estimated from the single-degenerate model. The third integral illustrates the contribution of stars in the mass range of $M_{Bm} - M_{BM}$, and the fourth integral is the contribution from core-collapse SNe.

Appendix F

The Simple Kinematic Model: Distribution of HVC Locations and Velocities

A three-dimensional coordinate system of (x, y, z) is defined with (x, y) as the galactic plane and the location of the Sun at $y = 0$. An HVC is considered located at (x, y, z) with a space velocity of (v_x, v_y, v_z) and we obtain,

$$r = \sqrt{x^2 + y^2} \tag{F.1}$$

$$d = \sqrt{(x - R_\odot)^2 + y^2 + z^2} \tag{F.2}$$

$$\theta = \arctan\frac{y}{x} \tag{F.3}$$

$$l = \pi + \arctan\frac{y}{x - R_\odot} \tag{F.4}$$

$$b = \arcsin\frac{z}{d} \tag{F.5}$$

$$v_r = +v_x\cos\theta + v_y\sin\theta \tag{F.6}$$

$$v_\theta = -v_x\sin\theta + v_y\cos\theta \tag{F.7}$$

$$\sin\alpha = \frac{R_\odot}{r}\sin l \tag{F.8}$$

$$\cos\alpha = \frac{r^2 + d^2 - R_\odot^2}{2rd} \tag{F.9}$$

$$v_{\rm GSR} = (v_r\cos\alpha - v_\theta\sin\alpha)\cos b + v_z\sin b \tag{F.10}$$

$$v_{\rm LSR} = v_{\rm GSR} + 220\sin l\cos b \tag{F.11}$$

where α, θ, r, and d are defined as the intermediate variables required for the estimation of the velocity of HVC relative to the GC, $v_{\rm GSR}$.

The mass of the HVC is estimated from a mass spectrum following a power-law,

$$N(M)\mathrm{d}M = N_o M^\alpha \mathrm{d}M \qquad \text{where} \quad M_{\rm low} < M < M_{\rm upp} \tag{F.12}$$

where $\alpha = -1.5$ [81], the upper mass limit for $M_{\rm upp}$ is 10^7 $\mathrm{M}_\odot$, and the density n is assumed to be in the range of $0.05 - 0.15$ cm^{-3} for the following relations.

By additionally converting the mass into an angular size, which in turn is translated to a brightness

temperature, we have,

$$R = (\frac{3M}{4\pi m_a \overline{n}})^{1/3} = 0.92(\frac{M}{10^6 \mathrm{M}_\odot})^{1/3}(\frac{\overline{n}}{0.01\mathrm{cm}^{-3}})^{-1/3}\mathrm{kpc} \tag{F.13}$$

$$\Omega = \pi(\frac{R}{D})^2 = \pi(318\mathrm{arcmin})^2(\frac{M}{10^6 \mathrm{M}_\odot})^{2/3}(\frac{\overline{n}}{0.01\mathrm{cm}^{-3}})^{-2/3}(\frac{D}{10\mathrm{kpc}})^{-2} \tag{F.14}$$

$$S = \frac{M(\mathrm{HI})}{0.236D^2} = \frac{2k}{10^{-26}\lambda^2}\sqrt{\frac{\pi}{4\ln 2}}WT_{B,p}\Omega \tag{F.15}$$

$$T_{B,p} = 0.59(\frac{f}{0.5})(\frac{M}{10^6 \mathrm{M}_\odot})^{1/3}(\frac{\overline{n}}{0.01\mathrm{cm}^{-3}})^{2/3}(\frac{W}{20\mathrm{km/s}})^{-1}(\frac{\min(\Omega, \Omega_{\mathrm{beam}})}{\Omega_{\mathrm{beam}}})\mathrm{K} \tag{F.16}$$

where M is the HVC mass in solar mass, f is the neutral fraction defined as $f = M(\mathrm{HI})/M(\mathrm{H})$, m_a is the average particle mass which is ~ 1.23 times heavier than the hydrogen atom including both the helium and the heavier elements in the mix, R is the radius of the HVC in the unit of kpc, D is the distance of the HVC from the Sun in the unit of kpc, Ω is the area in the unit of steradians, S is the profile integrated flux in the unit of Jy km s^{-1}, λ is the wavelength approximated as ~ 0.21 m, W is the full width half maximum (FWHM) of the velocity profile in the unit of km/s, T_B is the brightness temperature in the unit of K, and finally Ω_{beam} is for taking into account the beam dilution as it will reduce the observed T_B for unresolved HVCs.

From the model, it is estimated that the HVC complexes can fall towards the disk of the Milky Way at a net velocity of 50 km/s. Relative to the local standard of rest such velocity is translated to a range of velocities from -450 km/s up to $+300$ km/s. From such estimation, approximately 50% of the clouds would not be HVCs and the most negative velocity near $l = 90°$ would be $\sim$100 km/s which is larger than the positive velocity at $l = 270°$.

Appendix G

Physical Conditions for the Formation of a Galactic Fountain

With the assumption that there exists a source of hot gas such as SNe, under certain physical conditions a galactic fountain may occur [35, 36]. We define the mean atomic mass number m_a such as,

$$m_a = \sum_{elements} A_{el} m_{el} \sim 1.23 m_{\rm H} \tag{G.1}$$

where A_{el} is the abundance of an element, m_{el} is the atomic mass of an element, and $m_{\rm H}$ is the atomic mass of hydrogen. ($A(\rm H) = 0.925, A(\rm He) = 0.074$)

The mean particle mass, m_p, is estimated as $\sim 0.5 m_a$ in fully ionized gas at $T > 10^5$K. The mass density is calculated from m_a such as, $\rho = m_a n_{\rm H}$ and the pressure is estimated from m_p as, $P = \frac{\rho}{m_p} kT$. Then the sound speed c_s, can be estimated as,

$$c_s = (\frac{\gamma P}{\rho})^{1/2} = (\frac{\gamma k}{m_p})^{1/2}\, T^{1/2} \sim 67 (\frac{T}{10^{5.3}})^{1/2} \text{ km s}^{-1} \tag{G.2}$$

where $\gamma = 5/3$ represents the specific heat ratio. Given that the gravity above the stellar layer is $g_z = 6.25 \times 10^{-9}$cm s^{-2} [82], the ISM scaleheight, H, is estimated as following.

$$H = \frac{{c_s}^2}{g_z} \sim 2.3 (\frac{T}{10^{5.3}}) \text{kpc} \tag{G.3}$$

From the definitions, the dynamical timescale, $t_{\rm dyn}$ of the flow of gas is estimated as following.

$$t_{\rm dyn} = \frac{c_s}{g_z} \sim 34 (\frac{T}{10^{5.3}})^{1/2} (\frac{6.24 \times 10^{-9}}{g_z})^{-1} \text{ Myr} \tag{G.4}$$

On the other hand, the cooling timescale can be estimated from the rate of energy loss per unit mass, Q, and the rate of change in specific entropy, s, in a way such as,

$$\frac{{\rm D}s}{{\rm D}t} = \frac{Q}{T} \tag{G.5}$$

which can be further calculated with the standard interstellar cooling function, Λ. The cooling function is approximated by a power law above temperature $> 10^5$K and we obtain,

$$Q = \frac{\Lambda n_{\rm H}}{m_a} \text{ erg s}^{-1} \text{ g}^{-1} \tag{G.6}$$

$$\Lambda = 1.33 \times 10^{-19}\, T^{-1/2} \text{ erg cm}^3 \text{ s}^{-1} \tag{G.7}$$

The entropy of an ideal monatomic gas is known as,

$$S = Nk \log\{\frac{V}{N} (\frac{U}{N})^{3/2}\} + C \tag{G.8}$$

where C is just a constant, V is the volume, N is the number of particles, and $U = (3/2)NkT$ is the internal energy. From the definitions, $M = Nm_p$ and $\kappa = P\rho^{-5/3}$, the specific entropy, s, is calculated as,

$$s = \frac{S}{M} = \frac{k}{m_p}\log(\kappa^{3/2}) + C \tag{G.9}$$

where C here is a constant which is not necessarily equivalent to the constant in Equation (G.8). Further with the definition of κ and Ds/Dt, we have,

$$\frac{\mathrm{D}\kappa^{3/2}}{\mathrm{D}t} = \frac{-1.33 \times 10^{-19}\kappa^{1/2}}{m_a^2 m_p^{1/2}} = -q \tag{G.10}$$

where $q \sim 3.6 \times 10^{32}\mathrm{cm}^6\mathrm{g}^{-1}\mathrm{s}^{-4}$ can be used for estimating the radiative cooling time such as following.

$$t_{\mathrm{cool}} = \frac{\kappa^{3/2}}{q} = \frac{P^{3/2}}{q\rho^{5/2}} = \frac{k^{3/2}}{q m_p^{3/2} m_a}\frac{T^{3/2}}{n_{\mathrm{H}}} = 5.8(\frac{T}{10^{5.3}})^{3/2}(\frac{10^{-3}}{n_{\mathrm{H}}})\ \mathrm{Myr} \tag{G.11}$$

Then the ratio between the dynamical timescale and radiative cooling timescale, t_{cool} can be estimated as following.

$$\frac{t_{\mathrm{cool}}}{t_{\mathrm{dyn}}} = \gamma^{-1/2}\frac{P}{\rho^2}\frac{g_z}{q} \ \sim\ 0.17(\frac{T}{10^{5.3}})(\frac{10^{-3}}{n}) \tag{G.12}$$

Considering the environmental conditions close to the Sun, the cooling time will be a lot shorter than the dynamical time, $t_{\mathrm{cool}} << t_{\mathrm{dyn}}$. Under such condition, the hot gas will cool down before hydrostatic equilibrium and eventually fall down towards the galactic disk forming a galactic fountain.

References

[1] E. Kotoneva, C. Flynn, C. Chiappini, and F. Matteucci, "K dwarfs and the chemical evolution of the solar cylinder," *Monthly Notice of the Royal Astronomical Society*, vol. 336, pp. 879–891, 2002.

[2] A. N. M. Hulsbosch and B. P. Wakker, "A deep, nearly complete, survey of northern high-velocity clouds," *Astronomy and Astrophysics Supplement Series*, vol. 75, pp. 191–236, 1988.

[3] R. Morras, E. Bajaja, E. M. Arnal, and W. G. L. Pöppel, "A new survey for high velocity HI detections in the Southern Hemisphere," *Astronomy and Astrophysics Supplement*, vol. 142, pp. 25–30, 2000.

[4] D. D. Clayton, "Galactic chemical evolution and nucleocosmochronology - Standard model with terminated infall," *The Astrophysical Journal*, vol. 285, pp. 411–425, 1984.

[5] D. Lynden-Bell, "The chemical evolution of galaxies," *Vistas in Astronomy*, vol. 19, pp. 299–316, 1975.

[6] M. Tosi, "The effect of metal-rich infall on galactic chemical evolution," *Astronomy and Astrophysics*, vol. 197, pp. 47–51, 1988.

[7] C. Chiappini, F. Matteuci, and P. Padoan, "The chemical evolution of the galaxy with variable initial mass functions," *The Astrophysical Journal*, vol. 528, pp. 711–722, 2000.

[8] A. Maeder, "Stellar yields as a function of initial metallicity and mass limit for black hole formation," *Astronomy and Astrophysics*, vol. 264, pp. 105–120, 1992.

[9] M. Haywood, "A revision of the solar neighbourhood metallicity distribution," *Monthly Notices of the Royal Astronomical Society*, vol. 325, pp. 1365–1382, 2001.

[10] G. Malinie, D. H. Hartmann, D. D. Clayton, and G. J. Mathews, "Inhomogeneous chemical evolution of the Galactic disk," *The Astrophysical Journal*, vol. 413, pp. 633–640, 1993.

[11] R. J. Talbot and W. D. Arnett, "The Evolution of Galaxies. II. Chemical Evolution Coefficients," *The Astrophysical Journal*, vol. 186, pp. 51–67, 1973.

[12] P. Salucci, F. Walter, and A. Borriello, "ΛCDM and the distribution of dark matter in galaxies: A constant-density halo around DDO 47," *Astronomy and Astrophysics*, vol. 409, pp. 53–56, 2003.

[13] C. A. Muller, J. H. Oort, and E. Raimond, "Hydrogène neutre dans la couronne galactique?" *Comptes Rendus l'Academie des Sciences*, vol. 257, pp. 1661–1662, 1963.

[14] M. E. Putman, J. E. G. Peek, and M. R. Joung, "Gaseous Galaxy Halos," *Annual Review of Astronomy and Astrophysics*, vol. 50, pp. 491–529, 2012.

[15] C. Chiappini, F. Matteucci, and D. Romano, "Abundance Gradients and the Formation of the Milky Way," *The Astrophysical Journal*, vol. 554, pp. 1044–1058, 2002.

[16] K. H. Sung and K. Kwak, "Estimating the Fuel Supply Rate on the Galactic Disk from High-velocity Cloud (HVC) Infall," *The Astrophysical Journal*, vol. 881:4, 2019.

[17] M. Schmidt, "The Rate of Star Formation," *The Astrophysical Journal*, vol. 129, pp. 243–258, 1959.

[18] S. van den Bergh, "The frequency of stars with different metal abundances," *The Astrophysical Journal*, vol. 67, pp. 486–490, 1962.

[19] M. Schmidt, "The Rate of Star Formation. II. The Rate of Formation of Stars of Different Mass," *The Astrophysical Journal*, vol. 137, pp. 758–769, 1963.

[20] M. G. Edmunds and R. M. Greenhow, "General constraints on the effect of gas flows in the chemical evolution of galaxies - II. Radial flows and abundance gradients," *Monthly Notices of the Royal Astronomical Society*, vol. 272, pp. 241–264, 1995.

[21] B. P. Wakker, D. G. York, J. C. Howk, J. C. Barentine, R. Wilhelm, R. F. Peletier, H. van Woerden, T. C. Beers, Ž. Ivezić, and P. Richter, "Distances to Galactic High-Velocity Clouds: Complex C," *The Astrophysical Journal Letters*, vol. 670, no. 2, 2007.

[22] C. Thom, J. E. G. Peek, M. E. Putman, C. Heiles, K. M. G. Peek, and R. Wilhelm, "An Accurate Distance to High-Velocity Cloud Complex C," *The Astrophysical Journal*, vol. 684, no. 1, 2008.

[23] B. P. Wakker and H. van Woerden, "High-Velocity Clouds," *Annual Review of Astronomy and Astrophysics*, vol. 35, pp. 217–266, 2013.

[24] C. Chiosi, "Chemical evolution of the galactic disk - The inflow problem," *Astronomy and Astrophysics*, vol. 83, pp. 206–216, 1980.

[25] F. Matteucci and P. Francois, "Galactic chemical evolution : abundance gradients of individual elements," *Monthly Notices of the Royal Astronomical Society*, vol. 239, pp. 885–904, 1989.

[26] C. G. Lacey and S. M. Fall, "Chemical evolution of the galactic disk with radial gas flows," *The Astrophysical Journal*, vol. 290, pp. 154–170, 1985.

[27] C. Chiappini, F. Matteucci, and R. Gratton, "The Chemical Evolution of the Galaxy: The Two-Infall Model," *The Astrophysical Journal*, vol. 477, pp. 765–780, 1997.

[28] P. R. Shapiro and G. B. Field, "Consequences of a New Hot Component of the Interstellar Medium," *The Astrophysical Journal*, vol. 205, pp. 762–765, 1976.

[29] J. C. Houck and J. N. Bregman, "Low-Temperature Galactic Fountains," *The Astrophysical Journal*, vol. 352, p. 506, 1990.

[30] A. Rosen, J. N. Bregman, and M. L. Norman, "Hydrodynamical Simulations of Star-Gas Interactions in the Interstellar Medium with an External Gravitational Potential," *The Astrophysical Journal*, vol. 413, p. 137, 1993.

[31] M. A. de Avillez, "Disc-halo interaction — I. Three-dimensional evolution of the Galactic disc," *Monthly Notices of the Royal Astronomical Society*, vol. 315, pp. 479–497, 2000.

[32] M. K. R. Joung and M.-M. M. Low, "Turbulent Structure of a Stratified Supernova-driven Interstellar Medium," *The Astrophysical Journal*, vol. 653, pp. 1266–1279, 2006.

[33] K. Kwak, R. L. Shelton, and E. A. Raley, "The Evolution of Gas Clouds Falling in the Magnetized Galactic Halo: High-velocity Clouds (HVCs) Originated in the Galactic Fountain," *The Astrophysical Journal*, vol. 699, pp. 1775–1788, 2009.

[34] J. N. Bregman, "The galactic fountain of high-velocity clouds," *The Astrophysical Journal*, vol. 236, pp. 577–591, 1980.

[35] F. D. Kahn, *Investigating the universe.* Kluwer Academic Publishers, 1981.

[36] ——, "The temperature in very old supernova remnants," *Astronomy and Astrophysics*, vol. 50, pp. 145–148, 1976.

[37] L. Lu, B. D. Savage, K. R. Sembach, B. P. Wakker, W. L. W. Sargent, and T. A. Oosterloo, "The Metallicity and Dust Content of HVC 287.5+22.5+240: Evidence for a Magellanic Clouds Origin," *The Astrophysical Journal*, vol. 115, pp. 162–167, 1998.

[38] B. P. Wakker, T. A. Oosterloo, and M. E. Putman, "H I Fine Structure in Magellanic Tidal Debris," *The Astrophysical Journal*, vol. 123, pp. 1953–1970, 2002.

[39] B. K. Gibson, M. L. Giroux, S. V. Penton, M. E. Putman, J. T. Stocke, and J. M. Shull, "Metal Abundances in the Magellanic Stream," *The Astrophysical Journal*, vol. 120, pp. 1830–1840, 2000.

[40] L. T. Gardiner and M. Noguchi, "N-body simulations of the Small Magellanic Cloud and the Magellanic Stream," *Monthly Notices of the Royal Astronomical Society*, vol. 278, pp. 191–208, 1996.

[41] C. Mastropietro, B. Moore, L. Mayer, J. Wadsley, and J. Stadel, "The gravitational and hydrodynamical interaction between the Large Magellanic Cloud and the Galaxy," *Monthly Notices of the Royal Astronomical Society*, vol. 363, pp. 509–520, 2005.

[42] T. W. Connors, D. Kawata, and B. K. Gibson, "N-body simulations of the Magellanic Stream," *Monthly Notices of the Royal Astronomical Society*, vol. 371, pp. 108–120, 2006.

[43] J. N. Bregman and E. J. Lloyd-Davies, "X-Ray Absorption from the Milky Way Halo and the Local Group," *The Astrophysical Journal*, vol. 669, pp. 990–1002, 2007.

[44] B. Moore and M. Davis, "The origin of the Magellanic Stream," *Monthly Notices of the Royal Astronomical Society*, vol. 270, pp. 209–221, 1994.

[45] J. Grcevich and M. E. Putman, "H I in Local Group Dwarf Galaxies and Stripping by the Galactic Halo," *The Astrophysical Journal*, vol. 696, pp. 385–395, 2009.

[46] B. P. Wakker, J. C. Howk, B. D. Savage, H. van Woerden, S. L. Tufte, U. J. Schwarz, R. Benjamin, R. J. Reynolds, R. F. Peletier, and P. M. W. Kalberla, "Accretion of low-metallicity gas by the Milky Way," *Nature*, vol. 402, pp. 388–390, 1999.

[47] A. J. Fox, B. D. Savage, B. P. Wakker, P. Richter, K. R. Sembach, and T. M. Tripp, "Highly Ionized Gas Surrounding High-Velocity Cloud Complex C," *The Astrophysical Journal*, vol. 602, pp. 738–759, 2004.

[48] B. Fryxell, K. Olson, P. Ricker, F. X. Timmes, M. Zingale, D. Q. Lamb, P. MacNeice, R. Rosner, J. W. Truran, and H. Tufo, "FLASH: An Adaptive Mesh Hydrodynamics Code for Modeling Astrophysical Thermonuclear Flashes," *The Astrophysical Journal Supplement Series*, vol. 131, pp. 273–334, 2000.

[49] G. W. Rougoor, "The Neutral Hydrogen in the Central Region of the Galactic System," *Bulletin of the Astronomical Institutes of the Netherlands*, vol. 17, pp. 381–441, 1964.

[50] P. M. W. Kalberla and L. Dedes, "Global properties of the HI distribution in the outer Milky Way," *Astronomy and Astrophysics*, vol. 487, pp. 951–963, 2008.

[51] H. van Woerden, B. P. Wakker, U. J. Schwarz, and K. S. de Boer, *High-Velocity Clouds*. Springer, Dordrecht, 2005.

[52] C. Thom, M. E. Putman, B. K. Gibson, N. Christlieb, C. Flynn, T. C. Beers, R. Wilhelm, and Y. S. Lee, "The Galactic Nature of High-Velocity Cloud Complex WB," *The Astrophysical Journal*, vol. 638, pp. L97–L100, 2006.

[53] F. J. Lockman, R. A. Benjamin, A. J. Heroux, and G. I. Langston, "The Smith Cloud: A High-Velocity Cloud Colliding with the Milky Way," *The Astrophysical Journal Letters*, vol. 679, p. L21, 2008.

[54] S. Jin, "GCN: a gaseous Galactic halo stream?" *Monthly Notices of the Royal Astronomical Society: Letters*, vol. 408, pp. L85–L89, 2010.

[55] J. E. G. Peek, R. Bordoloi, H. Sana, J. Roman-Duval, J. Tumlinson, and Y. Zheng, "The First Distance Constraint on the Renegade High-velocity Cloud Complex WD," *The Astrophysical Journal Letters*, vol. 828, p. L20, 2016.

[56] G. Tenorio-Tagle, "The collision of clouds with the galactic disk," *Astronomy and Astrophysics*, vol. 94, p. 338, 1981.

[57] H. M. Lee, H. Kang, and D. Ryu, "Supersonic Collisions between Two Gas Streams," *The Astrophysical Journal*, vol. 464, pp. 131–140, 1996.

[58] M. V. del Valle, A. L. Müller, and G. E. Romero, "High-energy radiation from collisions of high-velocity clouds and the Galactic disc," *Monthly Notices of the Royal Astronomical Society*, vol. 475, pp. 4298–4308, 2018.

[59] K. Kwak, D. B. Henley, and R. L. Shelton, "Simulations of High-velocity Clouds. I. Hydrodynamics and High-velocity High Ions," *The Astrophysical Journal*, vol. 739, 2011.

[60] M.-M. M. Low, C. F. McKee, R. I. Klein, J. M. Stone, and M. L. Norman, "Shock Interactions with Magnetized Interstellar Clouds. I. Steady Shocks Hitting Nonradiative Clouds," *The Astrophysical Journal*, vol. 433, p. 757, 1994.

[61] T. W. Jones, D. Ryu, and I. L. Tregillis, "The Magnetohydrodynamics of Supersonic Gas Clouds: MHD Cosmic Bullets and Wind-swept Clumps," *The Astrophysical Journal*, vol. 473, p. 365, 1996.

[62] A. Santillán, J. Franco, M. Martos, and J. Kim, "The Collisions of High-Velocity Clouds with a Magnetized Gaseous Galactic Disk," *The Astrophysical Journal*, vol. 515, pp. 657–668, 1999.

[63] F. Comerón, *Infall of Gas in Galaxies and Triggered Star Formation. In: de Avillez M.A., Breitschwerdt D. (eds) From Observations to Self-Consistent Modelling of the ISM in Galaxies*. Springer, Dordrecht, 2004.

[64] J. M. Scalo, "The Stellar Initial Mass Function," *Fundamentals of Cosmic Physics*, vol. 11, pp. 1–278, 1986.

[65] B. A. Twarog, "The chemical evolution of the solar neighborhood. II - The age-metallicity relation and the history of star formation in the galactic disk," *The Astrophysical Journal*, vol. 242, pp. 242–259, 1980.

[66] H. J. Rocha-Pinto, W. J. Maciel, J. M. Scalo, and C. Flynn, "Age–Metallicity Relation and Star Formation History of the Galactic Disk," *Astrophysics and Space Science*, vol. 265, pp. 245–246, 1999.

[67] R. C. Kennicutt, "The rate of star formation in normal disk galaxies," *The Astrophysical Journal*, vol. 272, pp. 54–67, 1983.

[68] ——, "The Star Formation Law in Galactic Disks," *The Astrophysical Journal*, vol. 344, p. 685, 1989.

[69] N. C. Rana and D. A. Wilkinson, "An estimation of the radial distribution of molecular hydrogen in the Galaxy from the star formation rates," *Monthly Notices of the Royal Astronomical Society*, vol. 218, pp. 721–728, 1986.

[70] M. Tosi and A. I. Diaz, "Chemical Evolution of Spiral Galaxies - Models with Star Formation Proportional to Molecular Hydrogen," *Monthly Notices of the Royal Astronomical Society*, vol. 246, pp. 616–623, 1990.

[71] R. J. Talbot and W. D. Arnett, "The Evolution of Galaxies. IV. Highly Flattened Disks," *The Astrophysical Journal*, vol. 197, pp. 551–570, 1975.

[72] M. A. Dopita and S. D. Ryder, "On the law of star formation in disk galaxies," *The Astrophysical Journal*, vol. 430, pp. 163–178, 1994.

[73] A. Burkert and G. Hensler, "Anisotropic models of galactic evolution," *Astronomy and Astrophysics*, vol. 199, pp. 131–145, 1988.

[74] J. K{"oppen, C. Theis, and G. Hensler, "Self-regulated star-formation in chemodynamical models of galaxies," *Astronomy and Astrophysics*, vol. 296, pp. 99–109, 1995.

[75] G. E. Miller and J. M. Scalo, "The initial mass function and stellar birthrate in the solar neighborhood," *Astrophysical Journal Supplement Series*, vol. 41, pp. 513–547, 1979.

[76] F. X. Timmes, S. E. Woosley, and T. A. Weaver, "Galactic chemical evolution: Hydrogen through zinc," *Astrophysical Journal Supplement Series*, vol. 98, pp. 617–658, 1995.

[77] B. M. Tinsley, "Evolution of the stars and gas in galaxies," *Fundamentals of Cosmic Physics*, vol. 5, p. 287, 1980.

[78] V. Weidemann, "The initial-final mass relation - Galactic disk and Magellanic Clouds," *Astronomy and Astrophysics*, vol. 188, pp. 74–84, 1987.

[79] R. B. Larson, "Infall of Matter in Galaxies," *Nature*, vol. 236, pp. 21–23, 1972.

[80] S. Recchi, E. Spitoni, F. Matteucci, and G. A. Lanfranchi, "The effect of differential galactic winds on the chemical evolution of galaxies," *Astronomy and Astrophysics*, vol. 489, pp. 555–565, 2008.

[81] B. P. Wakker and H. van Woerden, "Distribution and origin of high-velocity clouds. III - Clouds, complexes and populations," *Astronomy and Astrophysics*, vol. 250, pp. 509–532, 1991.

[82] K. Kuijken and G. Gilmore, "The galactic disk surface mass density and the Galactic force K(z) at Z = 1.1 kiloparsecs," *The Astrophysical Journal Letters*, vol. 367, pp. L9–L13, 1991.